Published in "Newsletters on Stratigraphy 51 (3): 343–380, 2018"
which should be cited to refer to this work.

Age and synchronicity of planktonic foraminiferal bioevents across the Cenomanian–Turonian boundary interval (Late Cretaceous)

Francesca Falzoni[1]*, Maria Rose Petrizzo[1], Michèle Caron[2], R. Mark Leckie[3], and Khalifa Elderbak[3,4]

With 11 figures and 3 tables

Abstract. The upper Cenomanian–lower Turonian is a key-stratigraphic interval, as it encompasses the Late Cretaceous supergreenhouse and a major perturbation of the global carbon cycle (i.e., Oceanic Anoxic Event 2) as evidenced by a global positive carbon isotope excursion and by the nearly world-wide deposition of organic-rich marine facies. A turnover in planktonic foraminiferal assemblages and in other marine organisms is documented across this stratigraphic interval, but reconstruction of the timing and identification of the cause and effect relationships between environmental perturbations and organism response require a highly-resolved stratigraphic framework. The appearance and extinction levels of planktonic foraminiferal species generally allow accurate intra- and supra-basinal correlations. However, bioevents cannot be assumed to be globally synchronous, because the stratigraphic and geographic distribution of species is modulated by ecological preferences exhibited by each taxon and controlled by oceanic circulation, often resulting in earlier or delayed events in certain geographic areas (i.e., diachronous datums). The aim of this study is to test the synchronicity of the planktonic foraminiferal bioevents recognized across the C/T boundary and to provide the most reliable sequence of events for correlation of low to mid-latitude localities. For this purpose, we have compiled a highly-resolved biostratigraphic analysis of the European reference section for the C/T boundary at Eastbourne, Gun Gardens (UK), and core S57 (Tarfaya, Morocco), and correlated the sequence of bioevents identified with those recorded in other coeval sections available in the literature, including the GSSP section for the base of the Turonian Stage at Rock Canyon, Pueblo (Colorado), where we calculated reliable estimates of planktonic foraminiferal events that are well-constrained by radioisotopically and astrochronologically dated bentonite layers. Results indicate that the extinctions of *Thalmanninella deeckei*, *Thalmanninella greenhornensis*, *Rotalipora cushmani* and "*Globigerinelloides*" *bentonensis* in the latest Cenomanian are reliable bioevents for correlation. In addition, our analysis highlights other promising lowest occurrences (LOs) that need to be better constrained by bio- and chemostratigraphy, including the LO of *Marginotruncana schneegansi* falling close to the C/T boundary. By contrast, the appearance of *Helvetoglobotruncana helvetica* and of some *Dicarinella* species, the extinction of anaticinellids and the onset of the "*Heterohelix*" shift are likely diachronous across low to mid-latitude localities. Finally, our study suggests that different species concepts among authors, different sample size and sampling resolution, as well as species paleoecology are important factors that control the stratigraphic position at which bioevents are identified.

Key words. Cenomanian–Turonian, stratigraphy, mid-low latitude correlations, planktonic foraminifera, Pueblo, Eastbourne

Authors' addresses:
[1] Dipartimento di Scienze della Terra "A. Desio", Università degli Studi di Milano, via Mangiagalli 34, 20133 Milano, Italy.
[2] Département de Geosciences, Institut de Géologie, Université de Fribourg, Pérolles, 1700 Fribourg, Switzerland.
[3] Department of Geosciences, University of Massachusetts-Amherst, Amherst, Massachusetts 01003, USA.
[4] ALS Oil & Gas, 6510 Guhn Road, Houston, TX 77040, USA.
* Corresponding author: francesca.falzoni@unimi.it

1. Introduction

The Cenomanian–Turonian boundary interval (Late Cretaceous) represents one of the most interesting case-studies for investigating the evolution of the marine biota under the intense environmental perturbations that occurred during Oceanic Anoxic Event 2 (e.g., Schlanger and Jenkyns 1976, Scholle and Arthur 1980, Schlanger et al. 1987). In fact, OAE 2 is globally recognized as a time of increased sea-surface productivity under greenhouse climate conditions interrupted by a brief cooling episode (i.e., the "Plenus Cold Event", see Gale and Christensen 1996, Forster et al. 2007, Sinninghe Damsté et al. 2010, Jarvis et al. 2011, Jenkyns et al. 2017, Kuhnt et al. 2017) that may correspond to rising sea level and to a re-oxygenation event of bottom waters in the Western Interior Seaway (WIS) (i.e., the "Benthonic Zone": Eicher and Worstell 1970, Eicher and Diner 1985, Leckie 1985, Elderbak and Leckie 2016). Across OAE 2, planktonic foraminiferal assemblages underwent a substantial turnover due to the extinction of the single-keeled rotaliporids with umbilical supplementary apertures (genera *Rotalipora* and *Thalmanninella*) and to the appearance and progressive diversification of double-keeled taxa (genera *Dicarinella* and *Marginotruncana*), that dominated the assemblages until the Santonian (Robaszynski et al. 1990, 1993, Premoli Silva and Sliter 1999, Leckie et al. 2002, Petrizzo 2002, Falzoni et al. 2013, 2016a, Petrizzo et al. 2017). However, correlating stratigraphic sequences, discriminating global from local signals, and reconstructing the cause and effect relationships between environmental changes and organism response require a reproducible and highly-resolved stratigraphic framework. Unfortunately, the C–T boundary interval lacks magnetostratigraphic control, since it is within the Cretaceous Normal Superchron (e.g., Gradstein et al. 2012). Nevertheless, this interval is accompanied by a ~+2‰ to 4‰ excursion in both the $\delta^{13}C_{carb}$ and $\delta^{13}C_{org}$ resulting from the burial of organic matter during OAE 2 (e.g., Jenkyns 2010). The shape of the $\delta^{13}C$ profile with its typical peaks and troughs represents one of the most reproducible features of this stratigraphic interval, as it is synchronously registered in the marine and continental records, and it represents a powerful tool for global correlation (e.g., Pratt and Threlkeld 1984, Arthur et al. 1987, Tsikos et al. 2004, Jarvis et al. 2006, 2011, Jenkyns 2010, Joo and Sageman 2014).

Planktonic foraminiferal bioevents are routinely applied to correlate pelagic and hemipelagic successions, and their contribution to implement the accuracy and resolution of the Geologic Time Scale has been particularly important since the Early Cretaceous (e.g., Bralower et al. 1995, Premoli Silva and Sliter 1995, Caron et al. 2006, Coccioni and Premoli Silva 2015). However, despite the wide distribution of this group of pelagic organisms, each living/fossil species possesses ecologic preferences that may control its geographic and stratigraphic distribution. Consequently, planktonic foraminiferal bioevents cannot be assumed to be globally synchronous and their reliability for correlation requires testing with other relative dating techniques. For instance, the identification of the Cenomanian/Turonian boundary based on planktonic foraminiferal events only is problematic. In fact, the base of the Turonian Stage is formally defined by the lowest occurrence (LO) of the ammonite *Watinoceras devonense* at the GSSP section at Rock Canyon, Pueblo, Colorado (Kennedy et al. 2000, 2005). However, ammonites are often rare or absent in hemipelagic and pelagic successions, thus the identification of the C/T boundary in the absence of the primary marker is based on secondary bioevents, including the LO of *Helvetoglobotruncana helvetica* among planktonic foraminifera. However, the appearance of *H. helvetica* is known to be an unreliable event to approximate the base of the Turonian because of its diachronous occurrence, rarity in the lower part of its stratigraphic distribution, very transitional evolution from its ancestor *Helvetoglobotruncana praehelvetica*, and absence or very rare occurrence in epicontinental margin settings (e.g., Hart and Carter 1975, Carter and Hart 1977, Hart and Weaver 1977, Hart and Bigg 1981, Leckie 1985, Hilbrecht et al. 1986, Jarvis et al. 1988, Lipson-Benitah et al. 1988, Robaszynski et al. 1990, Kuhnt et al. 1997, Keller et al. 2001, Luciani and Cobianchi 1999, Tur et al. 2001, Petrizzo 2001, Holbourn and Kuhnt 2002, Caron et al. 2006, Mort et al. 2007, Desmares et al. 2007, Hart 2008, Gebhardt et al. 2010, Huber and Petrizzo 2014, Elderbak and Leckie 2016). Further complication is introduced by inconsistencies in the stratigraphic position of planktonic foraminiferal events, including the identification of LOs (lowest occurrences) and HOs (highest occurrences) of marker taxa (e.g., *Rotalipora cushmani*, *H. helvetica*) when the same section is studied by different authors (Pueblo: Eicher and Diner 1985, Leckie 1985, Leckie et al. 1998, Keller and Pardo 2004, Caron et al. 2006, Desmares et al. 2007, Elderbak and Leckie 2016; Eastbourne: Paul et al. 1999, Keller et al. 2001, Hart et al. 2002, Tsikos et al. 2004).

The aim of this study is to select the most reliable and reproducible sequence of planktonic foraminiferal bioevents across the C–T boundary interval by distinguishing between the most trustworthy isochronous bioevents from those that are more regional or diachronous in nature. The section of Eastbourne at Gun Gardens and core S57 (Tarfaya Basin) were here restudied at high-resolution to complement the planktonic foraminiferal data published in Tsikos et al. (2004). We developed a well-constrained age-model of Pueblo (Rock Canyon) to obtain numerical estimates of planktonic foraminiferal events recognized in the GSSP section. Subsequently, we tested the synchronicity of each bioevent by performing graphic correlations between Pueblo (Rock Canyon) and Eastbourne (Gun Gardens) and between Pueblo (Rock Canyon) and Tarfaya (core S57), and by comparing the stratigraphic position of each bioevent with respect to the peaks and troughs of the $\delta^{13}C$ profile in other low to mid-latitude localities, selected among those yielding the most complete stratigraphic record and a highly-resolved $\delta^{13}C$ profile. Italian sections are only briefly discussed, because of the absence of planktonic foraminifera in the black shale layers (e.g., Premoli Silva and Sliter 1995, Premoli Silva et al. 1999, Coccioni and Luciani 2004, 2005, Coccioni and Premoli Silva 2015), and the stratigraphic gap across the Bonarelli Level and time equivalent organic-rich facies (Gambacorta et al. 2015).

2. Materials and Methods

To document the sequence of planktonic foraminiferal bioevents across the C–T boundary interval, we have examined samples from (1) Eastbourne, Gun Gardens, UK, and (2) core S57 drilled in the Tarfaya Basin (Morocco), and paleogeographically located in the Anglo-Paris Basin and central Atlantic Ocean, respectively (Tsikos et al. 2004; Fig. 1). The Eastbourne section yields the most expanded C–T boundary interval of the English Chalk and represents the European reference section for the C/T boundary (Paul et al. 1999). Planktonic foraminifera have been the object of a number of studies (Paul et al. 1999, Keller et al. 2001, Hart et al. 2002, Tsikos et al. 2004) and the section at Gun Gardens has been restudied to verify discrepancies observed in the identification of species and position of the bioevents (including zonal markers). The sampling resolution adopted here for the biostratigraphic analysis is 20 cm throughout the section at Eastbourne, and between 20 and 50 cm at Tarfaya. Rock samples from core S57 (Tarfaya) and from the Plenus Marls Member (Eastbourne) have been processed with peroxide water to obtain washed residues. Novelty of this study compared to Tsikos et al. (2004) is introduced by the disaggregation of chalk samples from the Grey Chalk, Ballard Cliff and Holywell Members (Eastbourne) with acetic acid (80 %) and water (20 %) to obtain washed residues yielding well-pre-

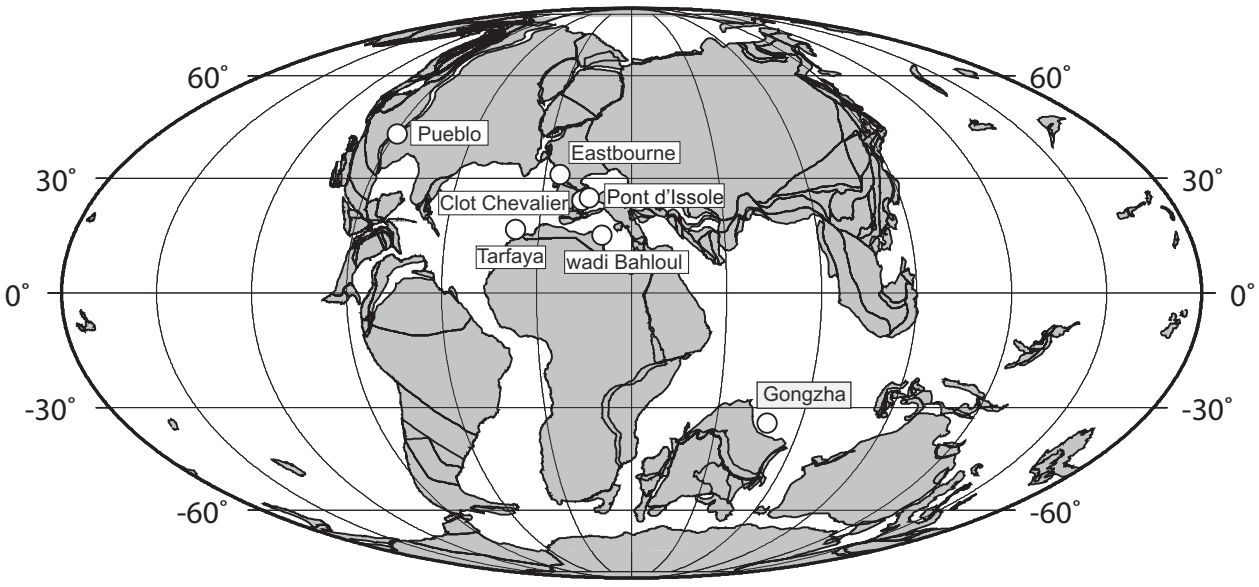

Fig. 1. Paleogeographic reconstruction for the late Cenomanian (94 Ma), with location of sections examined during this study (after Hay et al. 1999).

Table 1 Source of planktonic foraminiferal bioevents and biostratigraphy, methodology used to process samples, $\delta^{13}C_{carb}$ and $\delta^{13}C_{org}$ profiles available in the literature for each section treated in this study.

Sections	Planktonic foraminiferal bioevents and biostratigraphy	Methods for planktonic foraminiferal study	Available $\delta^{13}C_{carb}$ data (bulk)	Available $\delta^{13}C_{org}$ data (bulk)
Eastbourne	Paul et al. 1999	washed residues		
	Keller et al. 2001	washed residues		Paul et al. 1999
	Hart et al. 2002	not specified	Paul et al. 1999	Keller et al. 2001
	Tsikos et al. 2004	washed residues + thin sections	Tsikos et al. 2004	Tsikos et al. 2004
	this study	washed residues		
Tarfaya, core S57	Tsikos et al. 2004	washed residues	Tsikos et al. 2004	Tsikos et al. 2004
	this study	washed residues		
Pueblo	Eicher and Worstell 1970	washed residues	*Rock Canyon*:	*Rock Canyon*:
	Eicher and Diner 1985	washed residues	Caron et al. 2006;	Bowman and
	Leckie 1985	washed residues	*PU-79 Core*:	Bralower 2005;
	Leckie et al. 1998	washed residues	Pratt 1985;	*PU-79 Core*:
	West et al. 1998	washed residues	Pratt et al. 1993	Pratt and Threlkeld,
	Keller and Pardo 2004	washed residues	*Portland Core*:	1984; Pratt 1985;
	Caron et al. 2006	washed residues + thin sections	Sageman et al.	Pratt et al. 1993
	Desmares et al. 2007	washed residues + thin sections	2006	*Portland Core*:
	Elderbak and Leckie 2016	washed residues		Sageman et al. 2006
Clot Chevalier	Falzoni et al. 2016b	washed residues	Falzoni et al. 2016b	
Pont d'Issole	Grosheny et al. 2006	washed residues + thin sections	Grosheny et al. 2006 Jarvis et al. 2011	
wadi Bahloul	Caron et al. 2006	washed residues + thin sections	Caron et al. 2006	
Gongzha	Bomou et al. 2013	thin sections	Bomou et al. 2013	

served isolated specimens (see Lirer 2000 and Falzoni et al. 2016b for detailed procedure), a procedure also used by Elderbak and Leckie (2016) for the hard limestones at the Rock Canyon section.

In order to compare our biostratigraphic results with those from other localities, we have selected the most complete stratigraphic sequences spanning the C–T boundary interval with detailed planktonic foraminiferal biostratigraphic data, as well as a highly-resolved $\delta^{13}C_{carb}$ or $\delta^{13}C_{org}$ profile: WIS: (1) Rock Canyon, Pueblo, Colorado (Eicher and Diner 1985, Leckie 1985, Leckie et al. 1998, Keller and Pardo 2004, Caron et al. 2006, Desmares et al. 2007, Elderbak and Leckie 2016), Vocontian Basin: (2) Clot Chevalier (Falzoni et al. 2016b) and (3) Pont d'Issole (Grosheny et al. 2006), SE France; Tethyan Ocean: (4) wadi Bahloul, Tunisia (Caron et al. 2006); Indian Ocean: (5) Gongzha, Tibet (Bomou et al. 2013) (Fig. 1). In addition, planktonic foraminiferal bioevents identified at these localities are briefly discussed by comparing their stratigraphic position with other classic C/T boundary sections where the $\delta^{13}C$ profile is not available. The published litho-, bio-, and chemostratigraphic data of Clot Chevalier, Pont d'Issole, wadi Bahloul, and Gongzha are reproduced in the Supplementary Materials (Supplementary Figs. A–D). Sources of data for each section and the methodology applied to study the planktonic foraminifera (thin sections, washed residues or a combination of both) are listed in Table 1.

Taxonomic concepts for planktonic foraminiferal species identification follow their original descriptions and illustrations, the online taxonomic database for Mesozoic planktonic foraminifera "PF@Mikrotax" available at http://www.mikrotax.org/pforams/index.

html (see Huber et al. 2016), Robaszynski et al. (1979) and Falzoni et al. (2016b). Generic attribution is according to the taxonomic revision by González-Donoso et al. (2007) for rotaliporids and Haynes et al. (2015) for biserial taxa. Species mentioned in the text and/or in the figures are listed in the Taxonomic Appendix. The planktonic foraminiferal biozonation is according to Sliter (1989) and Robaszynski and Caron (1995).

3. Remarks on the planktonic foraminiferal record at Pueblo (Colorado)

The GSSP for the base of the Turonian Stage is located at the Rock Canyon section at Pueblo (Colorado). The primary marker for the identification of the base of the Turonian is the LO of the ammonite *Watinoceras devonense* in Bed 86 (Kennedy et al. 2000, 2005) (Fig. 2). According to the GSSP definition, additional secondary bioevents include the LO of the calcareous nannofossil *Quadrum gartneri*, which almost coincides with the C/T boundary as defined by ammonite stratigraphy at Pueblo (Tsikos et al. 2004), and the LO of the planktonic foraminifera *Helvetoglobotruncana helvetica* some distance above the C/T boundary.

Planktonic foraminifera at Pueblo have been studied numerous times over the last 45 years with different sampling resolution (Eicher and Worstell 1970, Eicher and Diner 1985, Leckie 1985, Leckie et al. 1998, Keller and Pardo 2004, Keller et al. 2004, Caron et al. 2006, Desmares et al. 2007, Elderbak and Leckie 2016). Almost all the above-mentioned studies [with the exception of Eicher and Worstell (1970), where the planktonic foraminiferal biozonation is not discussed] assigned the sedimentary succession outcropping at Rock Canyon to the three planktonic foraminiferal biozones according to the subtropical biozonation by Sliter (1989) and Robaszynski and Caron (1995): *R. cushmani*, *Whiteinella archaeocretacea* and *H. helvetica* Zones. However, some discrepancies can be found in the identification of the zonal markers, as follows: the HO of *R. cushmani* is identified in Bed 65 (Kennedy et al. 2005 after Eicher and Diner 1985), in Bed 66 (Keller and Pardo 2004), and within Bed 68 (Leckie 1985, Caron et al. 2006). Desmares et al. (2007) identified atypical morphotypes of *R. cushmani* (i.e., with a "discrete peripheral keel, which is sometimes not expressed on each chamber or is even totally absent") up to Bed 85. Leckie (1985) also reported a single occurrence of *R. cushmani* as high as the upper part of Bed 85, but with a significant stratigraphic gap between this and the presumed HO of *R. cushmani* in Bed 68 (below Bentonite A). The 3.5-m gap between relatively rare but consistently present *R. cushmani* up to Bed 68, followed by no specimens, and then extremely sparse presence in the upper part of Bed 85 begs a question about reworking.

There are also major inconsistencies with regard to the position of the LO of *H. helvetica*, which is identified in Bed 86 by Desmares et al. (2007), in Bed 89 by Keller and Pardo (2004) and Kennedy et al. (2005) after Eicher and Diner (1985), in Bed 102 by Caron et al. (2006), and in limestone Bed 103 by Elderbak and Leckie (2016). It should be noted here that three-dimensional specimens of foraminifera were extracted and analyzed from calcareous shales, marlstones, and limestones in the study by Elderbak and Leckie (2016). Based on the above, we placed the top of the *R. cushmani* Zone in Bed 68 according to Leckie (1985), representing the youngest record of the species, with the exception of the possibly reworked specimens within Bed 85, and the base of the *H. helvetica* Zone in Bed 103 according to Elderbak and Leckie (2016) (Fig. 2).

4. Re-interpretation of A, B, and C peaks on the $\delta^{13}C$ profile

Several $\delta^{13}C_{carb}$ and $\delta^{13}C_{org}$ records have been generated for the Rock Canyon section and for cores drilled nearby (PU-79 and Portland cores) over the last 30 years (Pratt and Threlkeld 1984, Pratt 1985, Pratt et al. 1993, Keller et al. 2004, Bowman and Bralower 2005, Caron et al. 2006, Sageman et al. 2006). In Fig. 2, we have plotted the $\delta^{13}C_{carb}$ obtained from outcrop samples at the GSSP section (Caron et al. 2006) and the $\delta^{13}C_{org}$ profile obtained from the PU-79 core (Pratt and Threlkeld 1984, Pratt 1985). The $\delta^{13}C_{org}$ curve by Pratt and Threlkeld (1984) and Pratt (1985) was later reproduced by other authors including Kennedy et al. (2005) in the paper where the GSSP for the base of the Turonian Stage was defined, with some discrepancies compared to the original version (see Caron et al. 2006 for discussion).

Pratt and Threlkeld (1984) and Pratt (1985) described peaks A, B, C as follows: "A = initial rapid increase in values and first peak; B = notch caused by brief decrease in values; C = second increase and

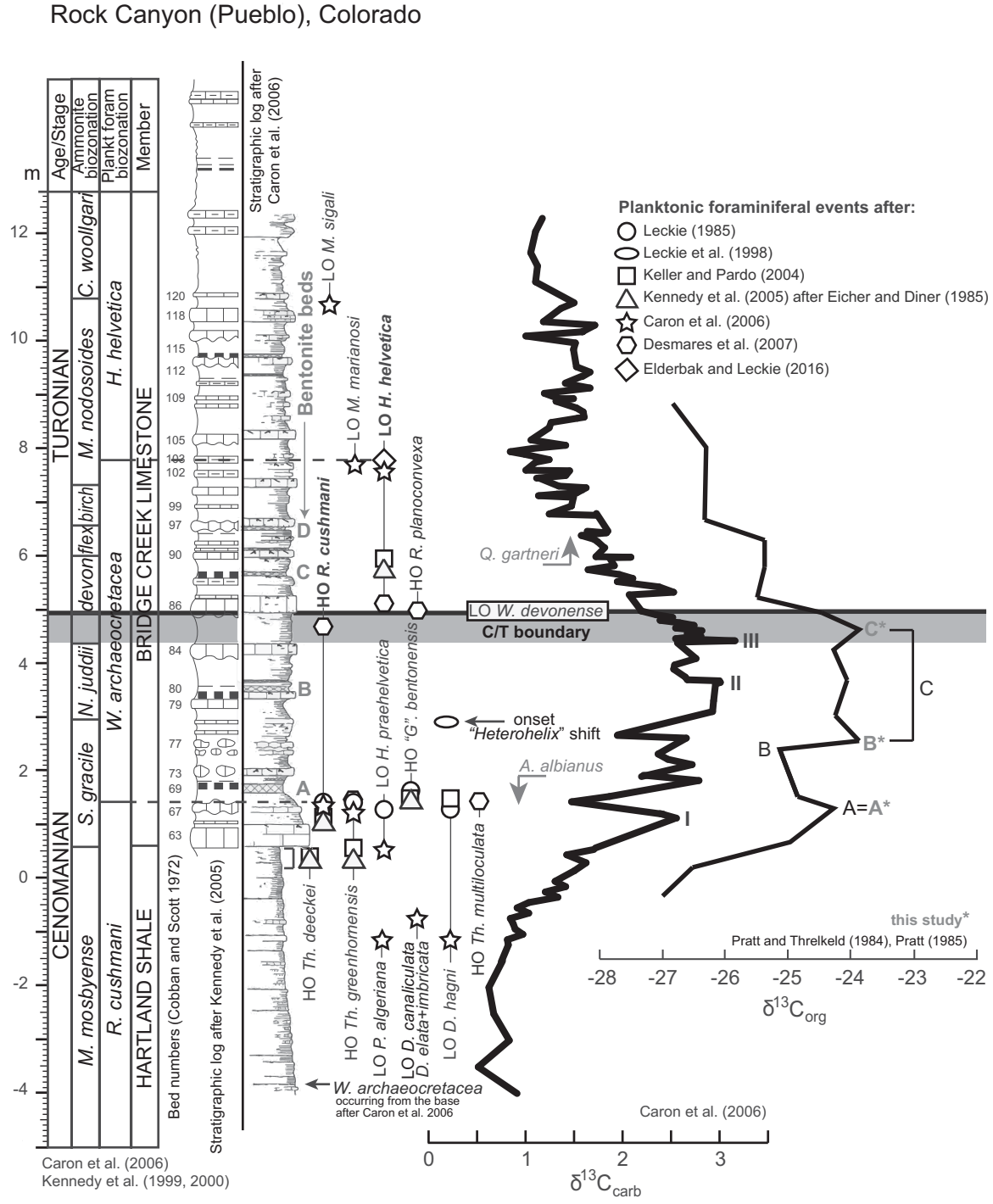

Fig. 2. Pueblo, Colorado (Western Interior Seaway). The C/T boundary is placed between the top of the *N. juddii* and the base of the *W. devonense* Zone according to Caron et al. (2006). Lithostratigraphy is from Kennedy et al. (2005) and stratigraphic logs with position of bentonites are from Kennedy et al. (2005) and Caron et al. (2006). Bed numbers are according to Cobban and Scott (1972). Ammonite biostratigraphy is after Kennedy et al. (1999, 2000). $\delta^{13}C_{carb}$ profile and position of peak I, II and III are after Caron et al. (2006). The $\delta^{13}C_{org}$ profile of the nearby PU-79 core (Pratt and Threlkeld 1984, Pratt 1985) is correlated with the Rock Canyon outcrop using marker beds. Planktonic foraminiferal bioevents are after Eicher and Diner (1985), Leckie (1985), Leckie et al. (1998), Keller and Pardo (2004), Caron et al. (2006), Desmares et al. (2007) and Elderbak and Leckie (2016). The top of the *R. cushmani* Zone is placed according to Leckie (1985), while the base of the *H. helvetica* Zone is according to Elderbak and Leckie (2016), see text for further explanations. Calcareous nannofossil events are after Tsikos et al. (2004). Abbreviations: LO = lowest occurrence, HO = highest occurrence.

plateau of values", meaning that Pratt and Threlkeld (1984) originally interpreted peak A as a maximum, peak B as a trough, and peak C as the entire plateau of positive (= less negative) values above B rather than a single point of the $\delta^{13}C$ profile (Fig. 2). However, different criteria have been successively adopted for the identification of the peaks first identified by Pratt and Threlkeld (1984). For instance, the position of the carbon isotope peaks in the Demerara Rise record (Erbacher et al. 2005; Leg 207, southern Caribbean) has been interpreted as follows: peaks A and B are troughs, C is the positive peak, and a fourth maximum point (named D) is recognized below the decrease of the $\delta^{13}C$ to pre-excursion values. By contrast, Jarvis et al. (2006, 2011) named A, B and C the three $\delta^{13}C_{carb}$ maxima across the C–T boundary interval in a composite isotope curve of the English chalk, with peak C falling very close to the C/T boundary. Voigt et al. (2007, 2008) adopted the same criteria but also recognized a fourth positive peak above the C/T boundary that they named D. These latter schemes were followed by a number of authors in recent years (e.g., Pearce et al. 2009, Westermann et al. 2010, Bomou et al. 2013, Eldrett et al. 2015, Falzoni et al. 2016b) resulting in the common practice of approximating the C/T boundary to point C (as interpreted by Jarvis et al. 2006) in the absence of *W. devonense*. Other authors preferred to number the observed maxima of the $\delta^{13}C$ profile as I, II, and III (e.g., Caron et al. 2006, Grosheny et al. 2006).

Based on the observations above, the position of the carbon isotope peaks A, B, and C is here summarized in order to univocally compare and correlate the planktonic foraminiferal bioevents across the stratigraphic sections discussed in this study. Therefore, considering previous interpretations, and according to Jarvis et al. (2006, 2011), we identify three positive points (A, B, C) and a plateau of high $\delta^{13}C_{carb}$ and $\delta^{13}C_{org}$ values, having a small offset, between B and C, and specifically, A is the initial rapid increase in values and first peak (as originally defined by Pratt and Threlkeld 1984, and Pratt 1985), B is the second positive peak of $\delta^{13}C$, following a decrease in values, and beginning of the plateau that is usually represented by multiple $\delta^{13}C$ points, and C is the last positive peak of the plateau before the carbon-isotope profile gradually decreases to pre-excursion values. Nevertheless, uncertainties might remain for the identification of A, B, C peaks in some localities, because of the presence of additional peaks and troughs due to local variations of the $\delta^{13}C$ content and/or to diagenesis that might complicate the apparently simple structure of the $\delta^{13}C$ profile and/or to a different sampling resolution. For instance, point C (i.e., the last positive peak of the plateau before the $\delta^{13}C$ decreases to pre-excursion values) at Eastbourne might be placed in two different positions, i.e., (1) at the transition between the Ballard Cliff and the Holywell Member according to Jarvis et al. (2006), or (2) near the top of the Ballard Cliff Member according to Voigt et al. (2008) (Fig. 3). Moreover, slight discrepancies in the stratigraphic position of peaks and troughs on the $\delta^{13}C_{carb}$ and $\delta^{13}C_{org}$ profiles are often observed in case both curves are available for the same section (e.g., Pueblo, Eastbourne).

5. Results

5.1 Eastbourne, Gun Gardens (UK)

Planktonic foraminiferal events identified at Eastbourne (Gun Gardens) in this study and those available in the literature (Paul et al. 1999, Keller et al. 2001, Hart et al. 2002, Tsikos et al. 2004) are combined with the available carbon isotope records (Paul et al. 1999, Tsikos et al. 2004) and plotted against stratigraphy (Fig. 3).

The HO of *R. cushmani* (Fig. 4, 1a–c) is recorded at top of Bed 3 (Keller et al. 2001) or within Bed 4 of the Plenus Marls Member (Paul et al. 1999, Hart et al. 2002, Tsikos et al. 2004), in agreement with this study, while the LO of *H. helvetica* is identified at the top of the Ballard Cliff (Keller et al. 2001) or at the base of the Holywell Member (Hart et al. 2002) (Fig. 3). By contrast, we do not record the occurrence of the latter species throughout the section, in agreement with Paul et al. (1999) and Tsikos et al. (2004). Discrepancies regarding the occurrence of *H. helvetica* at Eastbourne likely depend on different species concepts adopted by authors. However, confirmation of this hypothesis is complicated by the absence of figured specimens in Hart et al. (2002) and by the poor quality of the image of the *H. helvetica* specimen in Keller et al. (2001), which is illustrated only in spiral view. The presence of a keel throughout the last whorl is the distinctive feature of *H. helvetica* (Bolli 1945, Huber and Petrizzo 2014), a feature that is not visible in the specimen figured. Consequently, the succession studied is here assigned to the *R. cushmani* (from 0 to 11.4 m) and to the overlying *W. archaeocretacea* Zone (from 11.4 to 26 m) (Fig. 3), according to Tsikos et al. (2004).

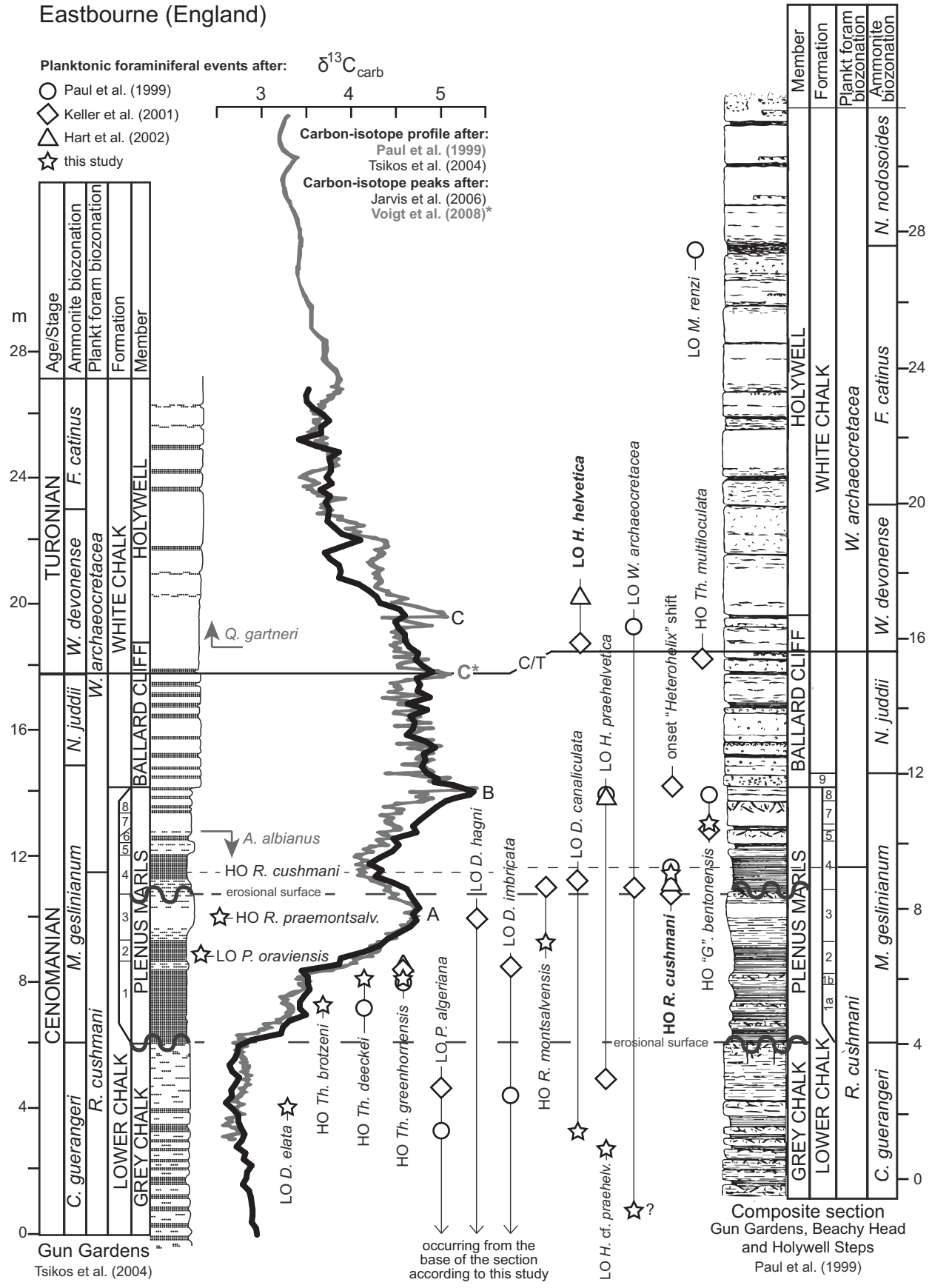

Based on our biostratigraphic analysis, *Praeglobotruncana algeriana* (Fig. 4, 2a–c), *Dicarinella hagni* (Fig. 4, 3a–c), and *Dicarinella imbricata* (Fig. 4, 4a–c) are present at the base of the section, therefore their LOs likely fall in older stratigraphic intervals (also supported by Huber et al. 1999 for *P. algeriana* and *D. hagni*). Moreover, we identified morphotypes resembling *H. praehelvetica* because of their distinctly flat spiral side that however never develop the keel on the first chambers of the last whorl throughout the stratigraphic interval studied. These morphotypes, here named *H.* cf. *praehelvetica* (Fig. 4, 5a–c), might represent very primitive or poorly developed specimens of *H. praehelvetica* and their LO is identified at 2.4 m above the base of the section (Fig. 3). Additional planktonic foraminiferal events identified in the Grey Chalk are listed below in stratigraphic order: 1) the LO of *Dicarinella canaliculata* at 3.2 m; and 2) the LO of *Dicarinella elata* (Fig. 4, 6a–c) at 4.0 m. The following events are identified in the Plenus Marls Member: 1) the HO of *Thalmanninella brotzeni* (Fig. 4, 7a–c) at 7.2 m above the base of the section; 2) the HO of *Thalmanninella greenhornensis* (Fig. 4, 8a–c) and of 3) *Thalmanninella deeckei* (Fig. 4, 9a–c) at 8.2 m within Bed 1; 4) the LO of *Praeglobotruncana oraviensis* (Fig. 4, 10a–c) at 8.8 m, and 5) the HO of *Rotalipora montsalvensis* (Fig. 5, 1a–c) at 9.2 m within Bed 2; 6) the HO of *Rotalipora praemontsalvensis* (Fig. 5, 2a–c) at 10 m within Bed 3; and 7) the HO of "*Globigerinelloides*" *bentonensis* at 13 m within Bed 7 (Fig. 3). Specimens that fall in the range of variability of *W. archaeocretacea* (Fig. 5, 3a–c) are identified from 0.6 m above the base of the section, but occur rarely in the assemblage and show an extremely scattered stratigraphic distribution, therefore their first appearance at 0.6 m may not correspond to its LO in the English Chalk. No noteworthy planktonic foraminiferal bioevents have been identified in the White Chalk Formation. The C/T boundary is here placed at the base of the *W. devonense* Zone according to Gale et al. (2005), however, it is worth mentioning that the ammonite species *W. devonense* is not identified at Eastbourne and the *W. devonense* Zone is recognized based on the occurrence of other coeval ammonite species (Paul et al. 1999, Gale et al. 2005).

5.2 Tarfaya (core S57)

The sedimentary succession studied is assigned to the *R. cushmani* (from the base of the core to 50.96 m) and to the overlying *W. archaeocretacea* Zone (from 50.96 m to the top of the cored interval), according to Tsikos et al. (2004). The occurrence of *H. helvetica* is not recorded in the stratigraphic interval examined (Fig. 6). Planktonic foraminiferal bioevents identified in this study are listed in stratigraphic order: (1) LO of *H. praehelvetica* (54.91 m) (Fig. 5, 4a–c), (2) HO of *Th. deeckei* (54.16 m) (Fig. 5, 5a–c), (3) HO of *Th. greenhornensis* (53.96 m) (Fig. 5, 6a–c), and (4) HO of "*G.*" *bentonensis* (50.16 m) (Fig. 5, 7a–b). The "*Heterohelix*" shift (abundance of biserial taxa $> 50\,\%$ in the > 63 µm size fraction *sensu* Leckie et al. 1998) is recorded from 50.55 m. Biserial taxa, mainly *Planoheterohelix moremani* (Fig. 5, 8a–b), *Planoheterohelix paraglobulosa* (Fig. 5, 9a–b) and *Planoheterohelix globulosa* dominate the assemblage up to the top of the core. *Praeglobotruncana algeriana* (Fig. 5, 10a–c), *Dicarinella hagni* (Fig. 5, 11a–c), and *Dicarinella imbricata* occur from the bottom of the core. The C/T boundary is here approximated between the peak C on the $\delta^{13}C_{org}$ profile and the LO of *Q. gartneri* according to Tsikos et al. (2004).

Fig. 3. Eastbourne (UK). On the left: lithostratigraphy, planktonic foraminiferal biostratigraphy and $\delta^{13}C_{carb}$ profile (black) after Tsikos et al. (2004), age/stage and ammonite biostratigraphy after Gale et al. (2005). On the right: age/stage, lithostratigraphy, planktonic foraminiferal and ammonite biostratigraphy after Paul et al. (1999). The $\delta^{13}C_{carb}$ profile (grey) is according to Paul et al. (1999) and refers to the stratigraphic log on the right. Chemostratigraphic peaks are after Jarvis et al. (2006) and Voigt et al. (2008) (see text for further details). The samples examined in this study refer to the stratigraphic log by Tsikos et al. (2004) in the left. Erosional basal surfaces are according to Keller et al. (2001). Calcareous nannofossil events are according to Tsikos et al. (2004). Planktonic foraminiferal events after Paul et al. (1999), Keller et al. (2001), Hart et al. (2002), and this study. Please note that the occurrence of *H. helvetica* and of the "*Heterohelix*" shift could not be confirmed by this study in agreement with Paul et al. (1999) and Tsikos et al. (2004). Also, we could not confirm the occurrence of specimens resembling the holotype of *H. praehelvetica*. Abbreviations: LO = lowest occurrence, HO = highest occurrence.

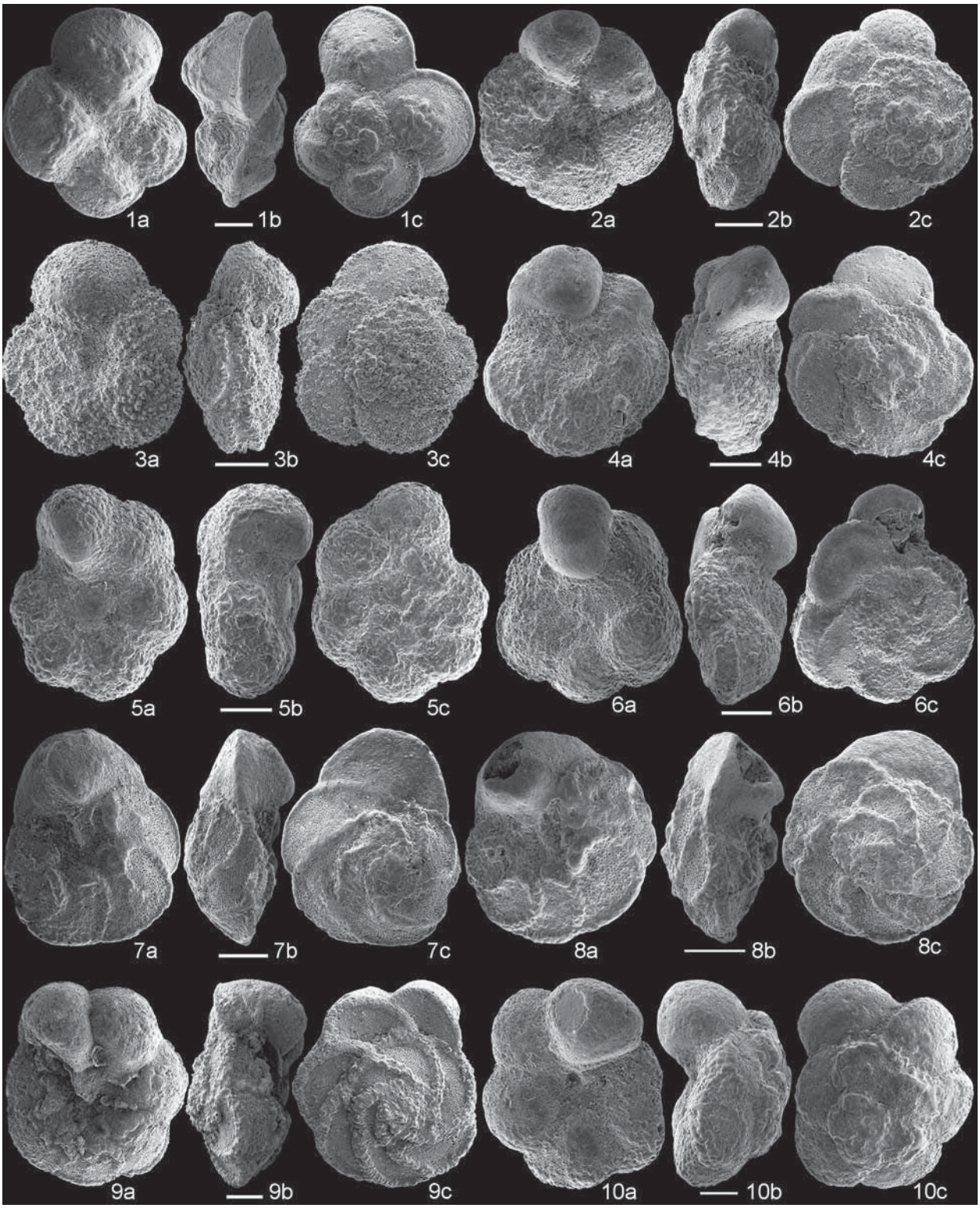

Fig. 4. Planktonic foraminiferal specimens from the Eastbourne section. (1a–c) *Rotalipora cushmani*, sample GC-600 (0 m, base of the section). (2a–c) *Praeglobotruncana algeriana*, sample GC-260 (3.4 m). (3a–c) *Dicarinella hagni*, sample WC1240 (26.3 m). (4a–c) *Dicarinella imbricata*, sample GC-480 (1.2 m). (5a–c) *Helvetoglobotruncana* cf. *praehelvetica*, sample PM+120 (7.2 m). (6a–c) *Dicarinella elata*, sample WC360 (17.5 m). (7a–c) *Thalmanninella brotzeni*, sample GC-340 (2.6 m). (8a–c) *Thalmanninella greenhornensis*, sample GC-260 (3.4 m). (9a–c) *Thalmanninella deeckei*, sample GC-260 (3.4 m). (10a–c) *Praeglobotruncana oraviensis*, sample PM+280 (8.8 m). Scale bar = 100 μm.

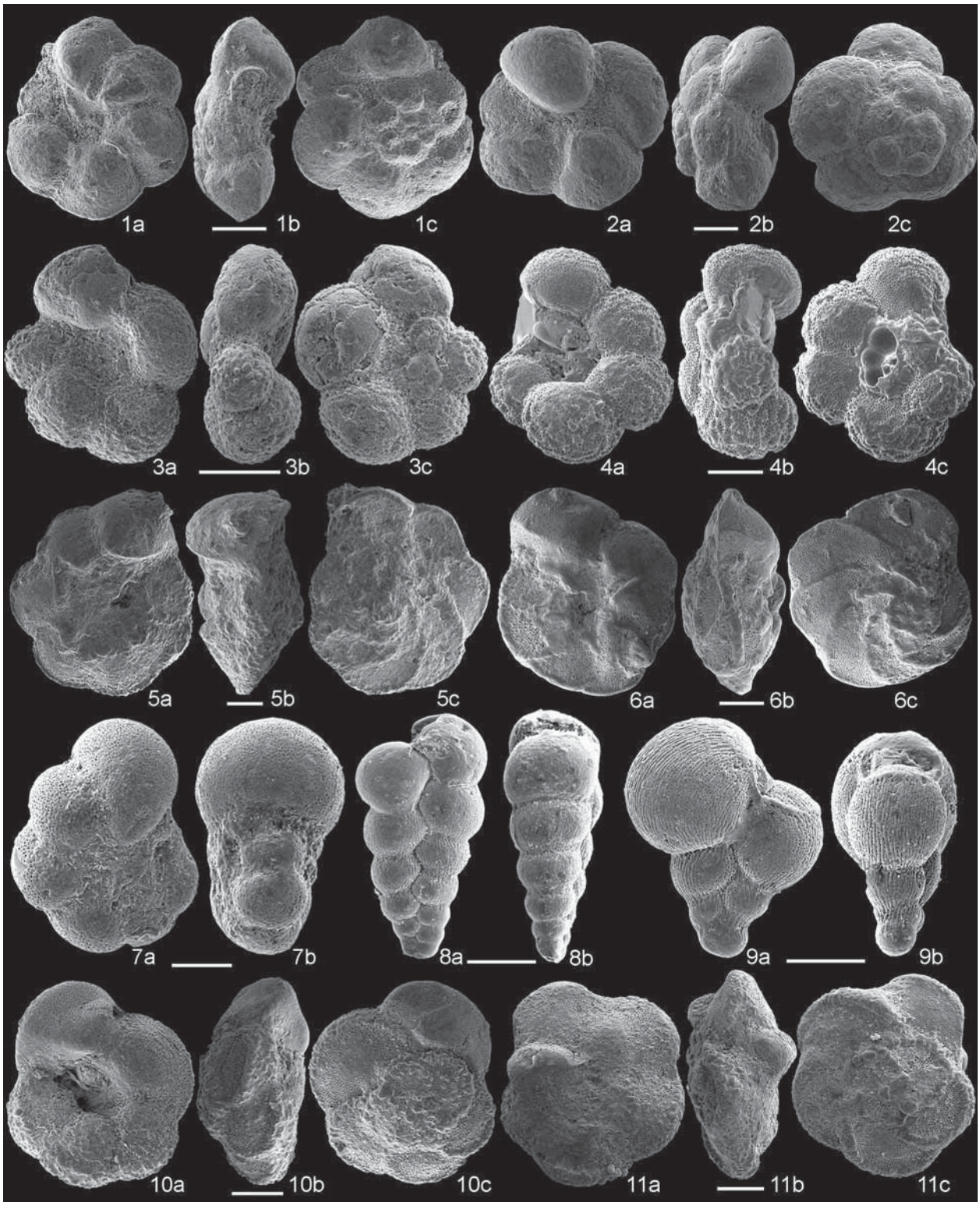

Fig. 5. Planktonic foraminiferal specimens from Eastbourne and Tarfaya. Eastbourne: (1a–c) *Rotalipora montsalvensis*, sample GC-500 (1 m). (2a–c) *Rotalipora praemontsalvensis*, sample PM+240 (8.4 m). (3a–c) *Whiteinella archaeocretacea*, sample GC-540 (0.6 m). Tarfaya: (4a–c) *Helvetoglobotruncana praehelvetica*, sample S57/T58, 45–51 cm (depth 57.25 m). (5a–c) *Thalmanninella deeckei*, sample S57/T59, 38–43 cm (depth 58.16 m). (6a–c) *Thalmanninella greenhornensis*, sample S57/T67, 9–14 cm (depth 59.55 m). (7a–b) *"Globigerinelloides" bentonensis*, sample S57/T59, 38–43 cm (depth 58.16 m). (8a–b) *Planoheterohelix moremani*, sample S57/T58, 45–51 cm (depth 57.25 m). (9a–b) *Planoheterohelix paraglobulosa*, sample S57/T58, 45–51 cm (depth 57.25 m). (10a–c) *Praeglobotruncana algeriana*, sample S57/T57, 61–66 cm (depth 56.50 m). (11a–c) *Dicarinella hagni*, sample S57/T57, 61–66 cm (depth 56.50 m). Scale bar = 100 μm.

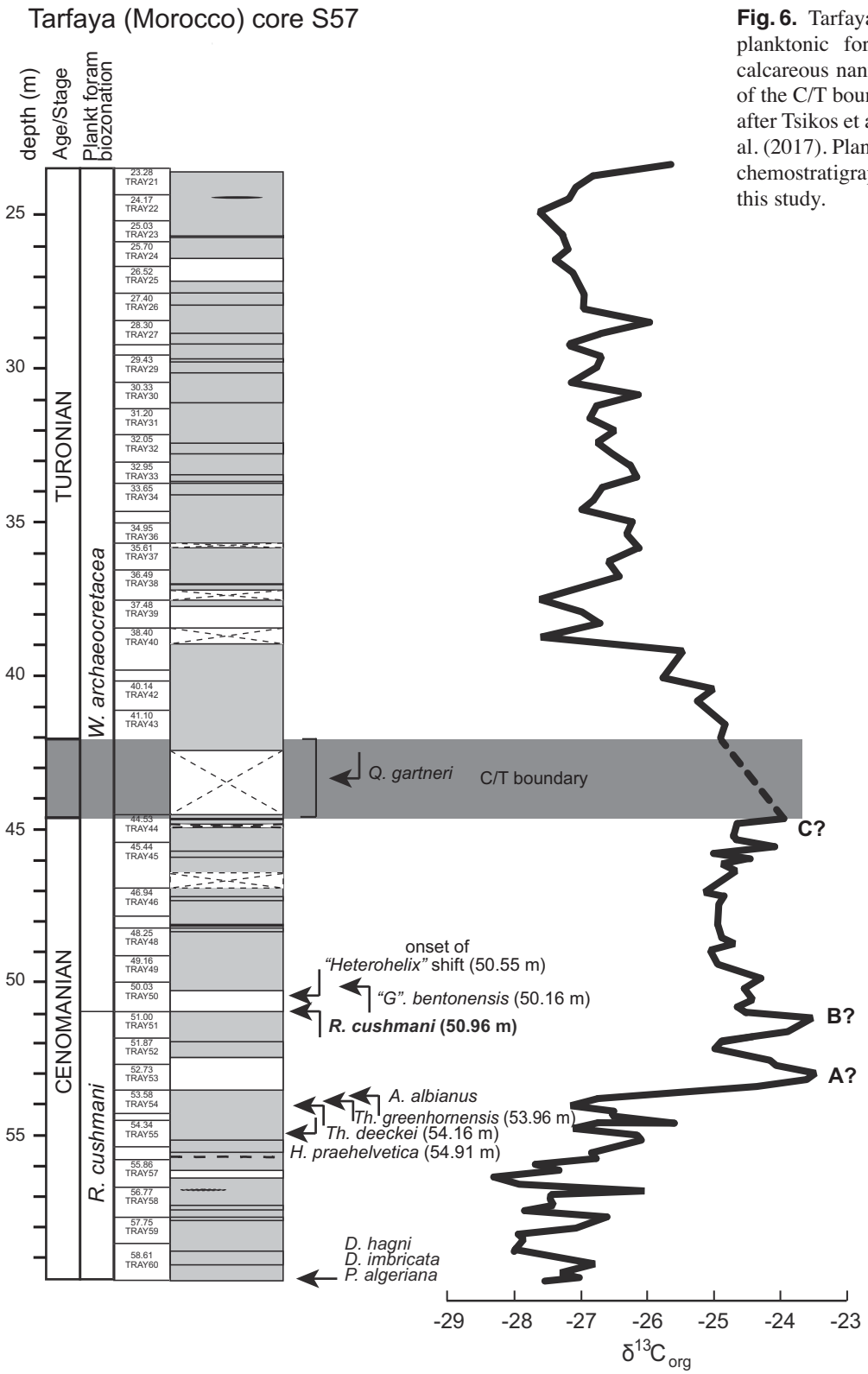

Fig. 6. Tarfaya, core S57 (Morocco): planktonic foraminiferal biozonation, calcareous nannofossil events, position of the C/T boundary and $\delta^{13}C_{org}$ profile after Tsikos et al. (2004) and Jenkyns et al. (2017). Planktonic foraminiferal and chemostratigraphic events according to this study.

6. Discussion

6.1 Age-depth model for the Pueblo section

Bentonites occurring in the Portland Core (Pueblo) were accurately and precisely dated by intercalibrating radioisotopic and astrochronologic time scales (Meyers et al. 2012). This study, and Elder (1988), also concluded that bentonites found in the same ammonite biozone in different localities of the WIS across the C–T boundary interval have a common eruptive origin and are isochronous. Therefore, we used the age of bentonites obtained by Meyers et al. (2012) to build the age-depth model for the Rock Canyon section and to calculate a reliable estimate of planktonic foraminiferal species first and last appearance data (Fig. 7). The age of the bentonites used to develop the age-model and the age of the bioevents extrapolated in this study are listed in Table 2. The calculated ages for the LO of *P. algeriana*, *D. hagni*, *D. elata*, *D. canaliculata*, and *D. imbricata*, the HO of *Th. deeckei*, and the LO of *H. praehelvetica* (base of the section) and the LO of *M. marianosi* and *H. helvetica* (top of the section) include a higher margin of error, because these events fall outside the interval constrained by bentonites, although they are aligned with the line of correlation. The age of the LO of *M. sigali* was not calculated, because it falls in an interval where the sedimentation rate might have been significantly different (see Fig. 2). The HO of *Th. multiloculata*, *R. planoconvexa* and atypical *R. cushmani* could not be calculated because of the unavailability of the precise sample depths at which these events are recognized.

The age obtained for the HO of *R. cushmani* (94.29 Ma) in this study is 10 kyr younger than the age reported in GTS 2012 (Gradstein et al. 2012) that was derived from the work by Robaszynski et al. (1998) in the Anglo-Paris Basin. Because the age estimate in the GTS 2012 was not well calibrated due to the uncertain HO of *R. cushmani* at Gubbio and in the Moroccan record (see Anthonissen and Ogg 2012), our calculated age for this event represents a more reliable estimate of its extinction across mid-low latitudes (see discussion in paragraph 6.3.1), as it falls very close to bentonite A. The LO of *H. helvetica* at 93.48 Ma is also slightly younger (40 kyr) than previously estimated by Huber and Petrizzo (2014), who obtained the age of 93.52 Ma at Pueblo using the age of bentonites by Meyers et al (2012), but entering the depth of the LO of *H. helvetica* according to Caron et al. (2006) instead of the depth revised by Elderbak and Leckie (2016) used in this study. The age of 93.52 Ma was also reported in GTS 2012 based on preliminary unpublished

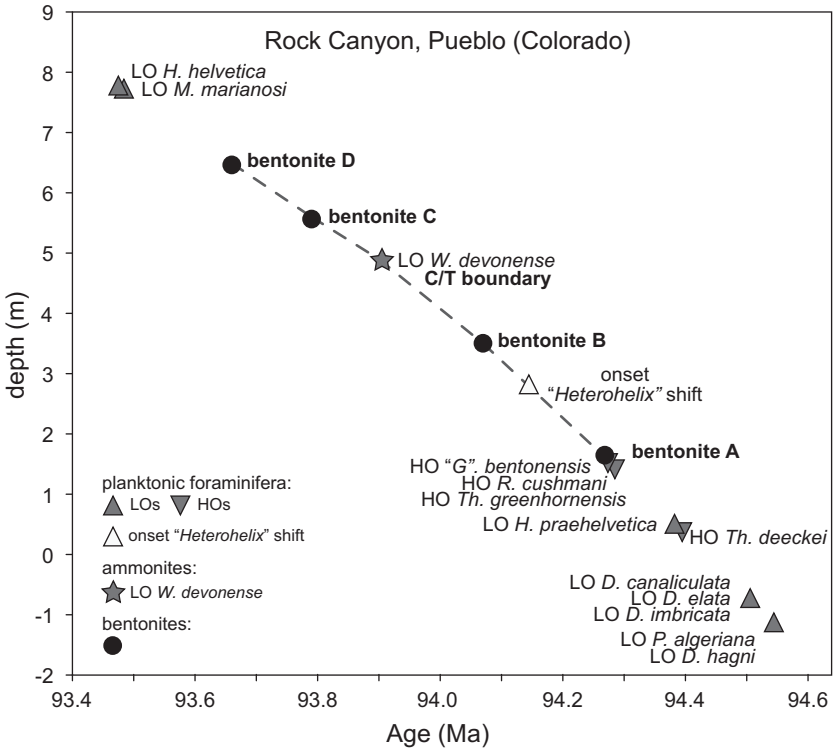

Fig. 7. Age-depth model for the Pueblo section. The age model is constrained by bentonite ages as calculated by Meyers et al. (2012). The linear functions obtained are as follows: 1) Bentonite A to Bentonite B ($y = -9.5x + 897.16$); 2) Bentonite B to LO of *W. devonense* ($y = -8.2353x + 778.19$); 3) LO of *W. devonense* to Bentonite C ($y = -6.3636x + 602.45$); 4) Bentonite C to Bentonite D ($y = -6.8462x + 647.7$).

data provided by Huber and Petrizzo (Gradstein et al. 2012). However, because of the clearly diachronous nature of this event, the age of 93.48 Ma obtained in this study cannot be applied to other localities. The LO of *D. imbricata* precedes the extinction of *R. cushmani* at Rock Canyon and in other localities (see discussion below) and the age derived for its appearance in the GSSP section (94.51 Ma) is significantly older (310 kyr) than estimated in the GTS 2012 (Gradstein et al. 2012), where this event is reported to occur above the HO of *R. cushmani*. Finally, it is worth noting that the extinction of *Th. greenhornensis* is significantly delayed at Pueblo compared to other mid-low latitude records (see paragraph 6.4.1), therefore the age obtained in this study has to be recalibrated in other localities.

6.2 Graphic correlations

To test the synchroneity of common events and the accuracy of correlations among sections, we performed graphic correlations of Pueblo *vs*. Eastbourne (Fig. 8a) and Pueblo *vs*. Tarfaya (Fig. 8b). This method has the advantage of clearly indicating which events occur earlier and which occur later in the sections compared, and highlights any variation in the sedimentation rates including the presence of hiatuses. For this reason, graphic correlations and the calculation of the correlation coefficient of the best-fit regression lines are routinely applied in biostratigraphic studies as a plain and simple tool to evaluate the synchroneity of events (e. g., Shaw 1964, MacLeod and Keller 1991, Sadler 2004, Paul and Lamolda 2009, Petrizzo et al. 2011, 2017, Lamolda et al. 2014, Smith et al. 2015, Huber et al. 2017, Olayiwola et al. 2017) and have been suggested as a standard procedure in any study aimed to select GSSP sections (Lamolda et al. 2014).

To increase the number of common events, we integrated planktonic foraminiferal datums with the calcareous nannofossil, ammonite, and chemostratigraphic events (peaks A, B and C of the $\delta^{13}C$ profile) available in the literature. Moreover, we considered the two interpretations regarding the position of peak C at Eastbourne (i.e., according to Jarvis et al. 2006 and to Voigt et al. 2008), in order to verify which option provides the highest correlation coefficient of the best-fit regression line. The depths of events used to constrain the graphic correlations and their sources are listed in Table 3. For the Pueblo section, we considered the youngest record for extinctions and the oldest record for appearances in case the same event was recognized in different positions by different authors, with the exception of the HO of *R. cushmani*, which is according to Leckie (1985).

Table 2 Mean depths and ages of the events constrained by the age-depth model for the Pueblo section. Mean depths are calculated as the average between the depth of the sample in which an event is identified and the depth of the underlying (for lowest occurrences) or overlying sample (for highest occurrences). Ages of bentonites and of the C/T boundary (LO of *W. devonense*) are from Meyers et al. (2012). The ages of the other bioevents are calculated in this study.

Rock Canyon, Pueblo (Colorado)		
Events	mean depth (m)	Age (Ma)
LO *H. helvetica*	7.75	93.48
LO *M. marianosi*	7.70	93.48
Bentonite D	**6.49**	**93.66**
Bentonite C	**5.60**	**93.79**
LO *W. devonense* – C/T boundary	**4.90**	**93.90**
Bentonite B	**3.50**	**94.07**
onset "*Heterohelix*" shift	2.80	94.14
Bentonite A	**1.60**	**94.27**
HO "*G.*" *bentonensis*	1.55	94.28
HO *Th. greenhornensis*	1.45	94.29
HO *R. cushmani*	1.45	94.29
LO *H. praehelvetica*	0.45	94.39
HO *Th. deeckei*	0.40	94.39
LO *D. canaliculata*	–0.75	94.51
LO *D. elata*	–0.75	94.51
LO *D. imbricata*	–0.75	94.51
LO *D. hagni*	–1.20	94.55
LO *P. algeriana*	–1.20	94.55

6.2.1 Pueblo vs. Eastbourne

We have excluded the HO of *Th. greenhornensis* to calculate the correlation coefficient of the regression line (R^2), because this event falls between peaks A and B of the $\delta^{13}C$ curve at Pueblo and below peak A at Eastbourne, thus is clearly delayed in the former section, as confirmed by the graphic correlation (Fig. 8a). The values of R^2 calculated using all the other common events identified at Pueblo and at Eastbourne are similar when considering peak C placed according to Jarvis et al. (2006) (R^2 = 0.90849) and according to Voigt et al. (2008) (R^2 = 0.92105). However, the graphic correlation highlights a possible variation in the sedimentation rate in one or both sections from around peak B, as testified by a change in the inclina-

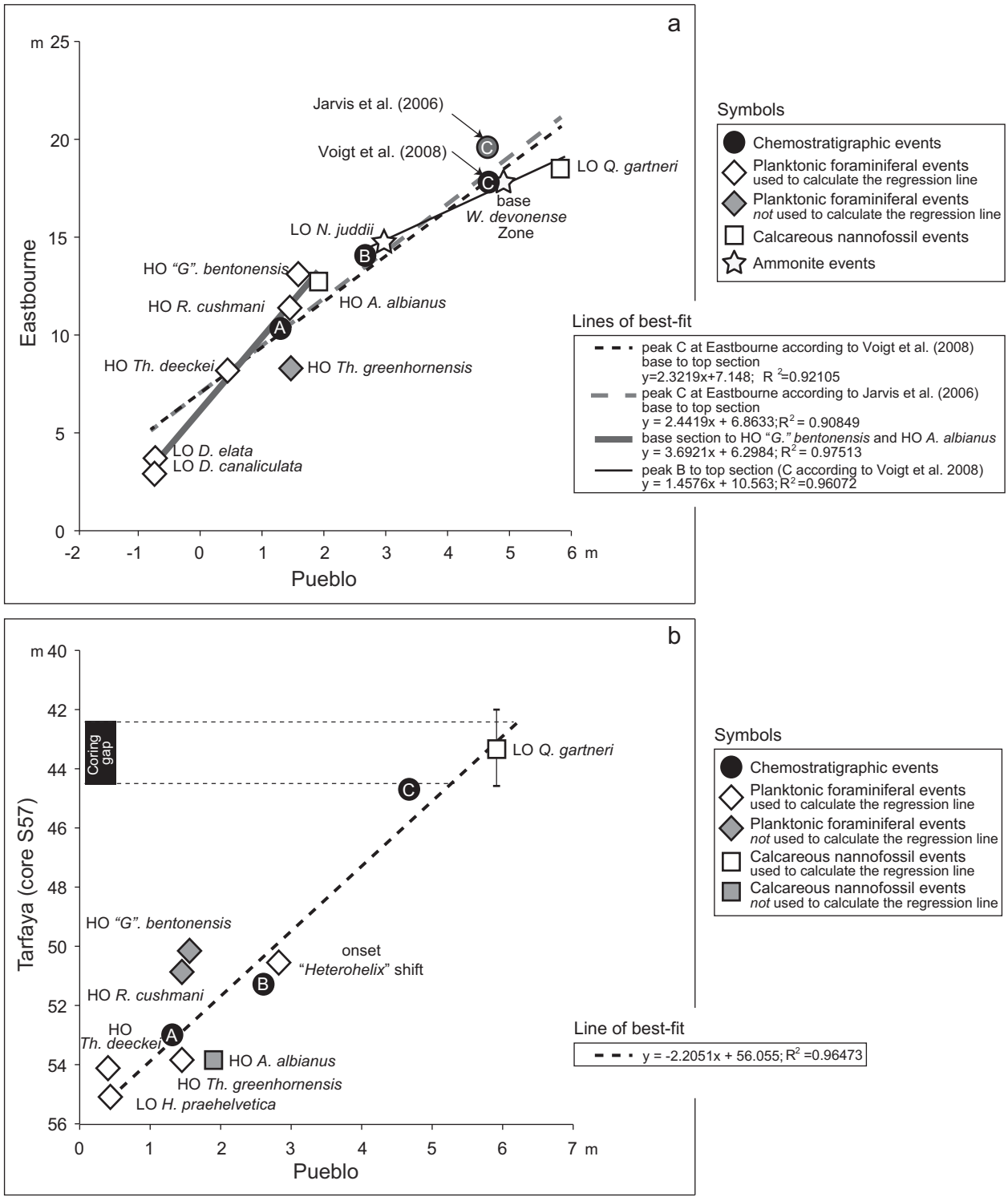

Fig. 8. Graphic correlations: 8a) Depth-depth plot of Pueblo vs. Eastbourne and 8b) depth-depth plot of Pueblo vs. Tarfaya (core S57). Please note that the depth of the LO of *Q. gartneri* at Tarfaya is represented with the error bar because its precise position is uncertain and likely falls within the coring gap (Tsikos et al. 2004).

Events	Mean depth (m)	Source
Pueblo		
LO *D. canaliculata*	−0.75	Caron et al. (2006)
LO *D. elata*	−0.75	Caron et al. (2006)
HO *Th. deeckei*	0.40	Eicher and Diner (1985)
LO *H. praehelvetica*	0.45	Caron et al. (2006)
δ^{13}C peak A	1.30	Pratt and Threlkeld (1984)
HO *Th. greenhornensis*	1.45	Leckie (1985)
HO *R. cushmani*	1.45	Leckie (1985)
HO "*G*". *bentonensis*	1.55	Leckie (1985)
HO *A. albianus*	1.90	Tsikos et al. (2004)
δ^{13}C peak B	2.60	Pratt and Threlkeld (1984)
onset "*Heterohelix*" shift	2.80	Leckie et al. (1998)
LO *N. juddii*	2.95	Caron et al. (2006)
δ^{13}C peak C	4.65	Pratt and Threlkeld (1984)
LO *W. devonense*	4.90	Caron et al. (2006)
LO *Q. gartneri*	5.85	Tsikos et al. (2004)
Eastbourne		
LO *D. canaliculata*	3.00	this study
LO *D. elata*	3.80	this study
HO *Th. deeckei*	8.30	this study
HO *Th. greenhornensis*	8.30	this study
δ^{13}C peak A	10.40	Jarvis et al. (2006)
HO *R. cushmani*	11.30	Tsikos et al. (2004)
HO *A. albianus*	12.80	Tsikos et al. (2004)
HO "*G*". *bentonensis*	13.10	this study
δ^{13}C peak B	14.10	Jarvis et al. (2006)
LO *N. juddii*	14.85	Gale et al. (2005)
δ^{13}C peak C	17.90	Voigt et al. (2008)
base *W. devonense* Zone	17.90	Gale et al. (2005)
LO *Q. gartneri*	18.60	Tsikos et al. (2004)
δ^{13}C peak C	19.70	Jarvis et al. (2006)
Tarfaya (core S57)		
LO *H. praehelvetica*	55.02	this study
HO *Th. deeckei*	54.06	this study
HO *Th. greenhornensis*	53.85	this study
HO *A. albianus*	53.85	Tsikos et al. (2004)
δ^{13}C peak A	52.92	this study
δ^{13}C peak B	51.13	this study
HO *R. cushmani*	50.86	Tsikos et al. (2004)
onset "*Heterohelix*" shift	50.55	this study
HO "*G*". *bentonensis*	50.09	this study
δ^{13}C peak C	44.61	this study
LO *Q. gartneri*	43.32	Tsikos et al. (2004)

Table 3 Mean depths and sources of bio- and chemostratigraphic events identified at Pueblo, Eastbourne and Tarfaya that were used to perform the graphic correlations illustrated in Fig. 8. Mean depths are calculated as the average between the depth of the sample in which an event is identified (indicated in the text, paragraphs 5.1 and 5.2) and the depth of the underlying (for lowest occurrences) or overlying sample (for highest occurrences).

tion of the line joining the events in the upper right of Fig. 8a. A significant decrease in the sedimentation rate in the upper part of the Eastbourne section is in agreement with the age model developed by Keller et al. (2001) and is likely due to a drop in the terrigenous input starting from the transition between the Plenus Marls Member (deposited during a sea-level lowstand) and the White Chalk Formation (deposited during a high-stand). A slight decrease in the sedimentation rate was also identified at Pueblo approximately at the same stratigraphic level (near the base of the ammonite *Neocardioceras juddii* Zone) (Meyers et al. 2001) in agreement with the age-depth model developed in this study. Based on the observations above, we calculated two regression lines as follows: (1) from the base of the sections to the HO of "*G*." *bentonensis* and (2) from peak B to the top of the sections, both having a high correlation coefficient (R^2 = 0.97 and R^2 = 0.96, respectively) (Fig. 8a). In the latter case, we used the position of peak C as identified by Voigt et al. (2008) because it falls much closer to the other events. Noteworthy, the two latter correlation coefficients might be higher than those obtained above because based on a lower number of data points (i. e., common events). However, the R^2 obtained entering peak C according to Voigt et al. (2008) is surely higher than the R^2 that would result from the same number of data points, but considering peak C according to Jarvis et al. (2006), because of the alignment of all the other common events (peak B, LO of *N. juddii*, base of the *W. devonense* Zone and LO of *Q. gartneri*; Fig. 8a). Accordingly, the interpretation of peak C applied herein for Eastbourne follows Voigt et al. (2008).

6.2.2 Pueblo vs. Tarfaya (core S57)

The graphic correlation highlights many differences in the position of the events (Fig. 8b). Firstly, the δ^{13}C peaks are not perfectly aligned, suggesting a decrease in the sedimentation rate from peak B to peak C at Pueblo or an increase at Tarfaya, and/or an erroneous

interpretation of their position on the $\delta^{13}C_{org}$ profile at Tarfaya that is probably affected by diagenetic alteration as observed for the $\delta^{13}C_{carb}$ record (Tsikos et al. 2004). The presence of a 3-m thick coring gap and only two common events in the upper part of the sections, including the LO of *Q. gartneri* that likely falls within the non-recovery interval, complicates its interpretation (Fig. 8b).

Discrepancies are also found in the planktonic foraminiferal and calcareous nannofossil data, and the only events that appear trustworthy for correlation between Pueblo and Tarfaya are the LO of *H. praehelvetica* and the extinctions of *Th. deeckei* and *Th. greenhornensis*, as well as the onset of the "*Heterohelix*" shift. By contrast, the HO of *A. albianus* is delayed at Pueblo or falls in an earlier stratigraphic interval at Tarfaya, while the opposite is true for the HO of *R. cushmani* and of "*G.*" *bentonensis*, therefore these three events were not used to calculate the regression line.

Because of the uncertainties regarding the position of the $\delta^{13}C$ peaks and the few number of common events at the top of the stratigraphic interval studied, the evaluation of the reliability of planktonic foraminiferal events for correlation between Pueblo and Tarfaya requires further study and comparison with sections elsewhere. However, the synchronicity of bioevents in the Tarfaya Basin and their reliability for mid-low latitude correlations are more widely discussed in paragraph 6.3.1.

6.3 Testing the accuracy of mid-low latitude correlations using planktonic foraminifera

In order to compare all the sections available and with the attempt to test the reliability of bioevents for correlating low to mid-latitude localities, we used the $\delta^{13}C$ isotope excursion, assuming that it was synchronously registered in the sedimentary successions. We have plotted in Fig. 9 the planktonic foraminiferal bioevents herein identified at Eastbourne and Tarfaya and those documented from the selected stratigraphic sections (Pueblo, Clot Chevalier, Pont d'Issole, wadi Bahloul and Gongzha) against a schematic $\delta^{13}C$ profile. At Pueblo, the bioevents are placed according to their position with respect to the $\delta^{13}C_{org}$ curve by Pratt and Threlkeld (1984) with peaks as identified in this study. A summary of the most reliable sequence of planktonic foraminiferal bioevents resulting from our study is reproduced in Fig. 10.

6.3.1 Reliability of zonal markers

The extinction of *R. cushmani* at Pueblo is recorded in slightly different stratigraphic intervals: from slightly below to slightly above A on the $\delta^{13}C$ curve. However, robust data based on both thin sections and washed residues place the HO of *R. cushmani* above peak A on the $\delta^{13}C_{org}$ curve (Table 1; Leckie 1985, Leckie et al. 1998, Caron et al. 2006, Elderbak and Leckie 2016). Remarkable is the identification of atypical *R. cushmani* at Pueblo up to peak C (Leckie 1985, Desmares et al. 2007), representing the youngest record of morphotypes falling within the range of variability of *R. cushmani* documented in the literature (Fig. 9). The HO of *R. cushmani* is diachronous from south to north within the WIS (Frush and Eicher 1975, Leckie 1985, Desmares et al. 2007, Lowery et al. 2014), which is not surprising because of the local variations in the salinity, sea-surface temperatures and productivity, and the relatively shallow water depth (e.g., Caldwell and Kauffman 1993, Arthur et al. 1985, Pratt 1984, 1985, Leckie 1985, Leckie et al. 1998, Pagani and Arthur 1998, West et al. 1998, Keller et al. 2004, Corbett and Watkins 2013, Lowery et al. 2014, Elderbak et al. 2014, Elderbak and Leckie 2016, among many others) that might have favored the survival of the last representatives of *R. cushmani* in certain areas of the WIS and caused an earlier extinction in others. Moreover, the diachronous extinction of *R. cushmani* in the WIS does not result from its dilution by the bloom of other species, because it cannot be overlooked in the assemblages even if rare thanks to its distinctive morphology, and because its diachronous extinction in the WIS is known from the work by Frush and Eicher (1975) and has been recently confirmed by other authors in highly-resolved biostratigraphic studies of different sections (e.g., Desmares at al. 2007, Lowery et al. 2014, Lowery and Leckie 2017).

In the other sections examined, the HO of *R. cushmani* is typically recorded at peak A or between peak A and B, with the exception of Clot Chevalier and Tarfaya. In the former section, this event falls in an earlier stratigraphic interval (below A) due to a combination of causes: (1) the presence of a hiatus at the base of the Thomel Level and of an overlying condensed stratigraphic interval, and (2) the rarity of *R. cushmani* toward the top of its stratigraphic range, so that a possible hiatus or low sedimentation rate in this interval might considerably bias the position of its HO (Falzoni et al. 2016b). A more reliable HO of *R. cushmani* in the Vocontian Basin is identified at Pont d'Issole in between peaks A and B (Grosheny et al. 2006, Grosheny et al. 2017).

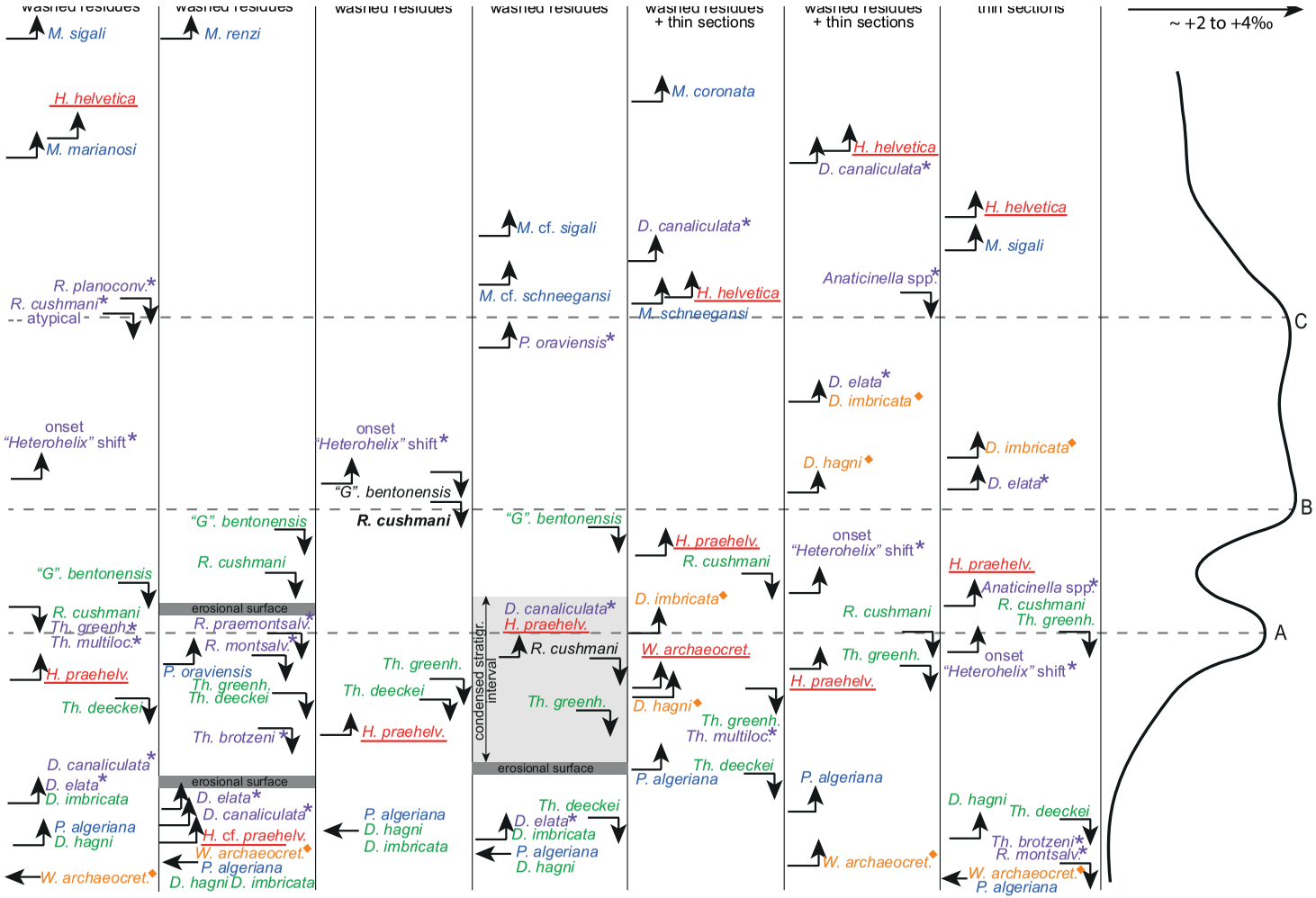

Fig. 9. Planktonic foraminiferal bioevents identified in each section plotted against a simplified $\delta^{13}C$ profile. The methodology applied to study planktonic foraminifera (washed residues and/or thin sections) is indicated for each locality. Pueblo = events that are identified in different position by different authors are placed as follows: the HOs of *Th. greenhornensis*, *R. cushmani* and "*G.*" *bentonensis* are according to Leckie (1985), the HO of *H. helvetica* is according to Elderbak and Leckie (2016), while all other events are placed following Caron et al. (2006), see text for further explanations. Events identified at Eastbourne are placed according to our study. The LO of *M. sigali* at Pueblo and the LO of *M. renzi* at Eastbourne fall well above the end of the $\delta^{13}C$ excursion in a younger stratigraphic interval. Reliable bioevents are in green, potentially useful bioevents are in blue. Misleading bioevents include (1) ecologically controlled bioevents (purple with star*), (2) unreliable bioevents because of taxonomic uncertainties, subjective species concepts and transitional evolution from ancestor species (red underlined), and (3) possibly delayed appearances because of species rare occurrence, low sampling resolution and/or small sample size (orange with diamond ♦). Misleading bioevents are categorized according to the most important factor that in our opinion controlled species diachronism, in case multiple options are possible. The HO of *R. cushmani* at Clot Chevalier is in black because its position is controlled by the sedimentologic features of the section. The HO of *R. cushmani* and "*G.*" *bentonensis* at Tarfaya are in black, because of the unreliability of the position of peak B on $\delta^{13}C_{org}$ profile. See text for references and discussion.

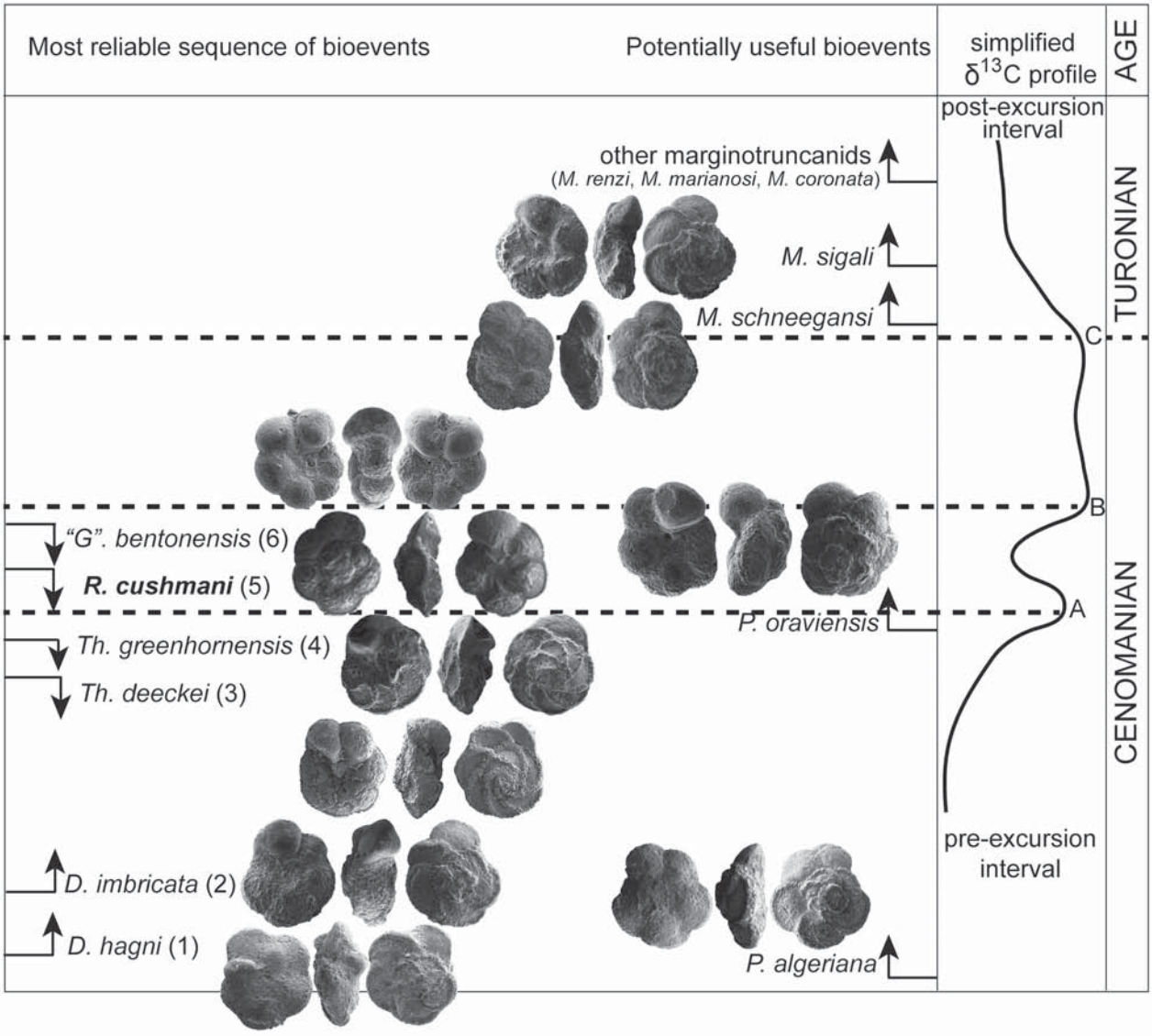

Fig. 10. Summary of the most reliable sequence of planktonic foraminiferal bioevents for mid-low latitude correlation across the C–T boundary interval and list of the bioevents that are potentially useful but require further calibration in other localities. Reliable bioevents are numbered in stratigraphic order from the bottom to the top.

The extinction of *R. cushmani* is recorded at Tarfaya (core S57) a few cm above the supposed peak B, while it falls between peak A and B in other cores drilled in the Tarfaya Basin (core S75: Kuhnt et al. 2005; core SN°4: Kuhnt et al. 2017). Specifically, the acquisition of highly-resolved bio- and chemostratigraphic data from a recently drilled core (SN°4) in the Tarfaya Basin indicates that the HO of *R. cushmani* falls in the trough between peak A and peak B (Kuhnt et al. 2017) as found in the other mid-low latitude localities. Therefore, its apparently delayed extinction in core S57, as well as that of "*G.*" *bentonensis*, more likely result from local environmental patterns and/or from a diagenetically altered $\delta^{13}C_{org}$ record, as explained in paragraph 6.2.2. On the other hand, we cannot completely rule out the possibility that differences in the paleobathymetry of cores S57, S75 and SN°4, approximately representing between 100 and 300 m (Kuhnt et al. 1990, 2005, 2017), might have influenced the timing of extinction of the deep-dweller *R. cushmani* (Hart 1999, Premoli Silva and Sliter 1999), although Kaiho et al. (2014) demonstrated that the extinction level of rotaliporids along a bathymetric transect was independent from water depth in the Spanish record.

The appearance of *H. helvetica* is recorded in different stratigraphic intervals above peak C at Pueblo, Pont d'Issole, wadi Bahloul and Gongzha. *Helvetoglobotruncana helvetica* is not identified at Clot Chevalier (Falzoni et al. 2016b), at Eastbourne and in core S57, in agreement with Tsikos et al. (2004). However, the LO of *H. helvetica* is documented in younger stratigraphic intervals at Tarfaya well above the C/T boundary (Kuhnt et al. 1990), further confirming its delayed occurrence in several localities. These observations support the unreliability of the LO of *H. helvetica* as a marker event for the base of the Turonian, as explained in the Introduction section.

6.4 Secondary planktonic foraminiferal bioevents for mid-to-low latitude correlations

6.4.1 Reliable bioevents

Extinctions across the C–T boundary interval follow a well-defined scheme that is reproducible in all the stratigraphic sections examined, as listed below in stratigraphic order: 1) HO of *Th. deeckei*, 2) HO of *Th. greenhornensis*, overlaid by the HO of *R. cushmani*, and by 3) the HO of "*G.*" *bentonensis* (Figs. 9–10).

1) The extinction of *Th. deeckei* always falls below peak A on the $\delta^{13}C$ curve, approximately at the beginning of the $\delta^{13}C$ excursion (Clot Chevalier, Pont d'Issole and Gongzha) or in a slightly younger stratigraphic interval where the $\delta^{13}C$ increases more distinctly (Pueblo, Eastbourne, Tarfaya).

2) The HO of *Th. greenhornensis* falls slightly below or at peak A, with the exception of Pueblo, where it falls slightly above peak A and together with the HO of *R. cushmani*, suggesting a delayed extinction in the WIS compared to the other mid-low latitude localities. Limited discrepancies in the HO of *Th. greenhornensis* and *Th. deeckei* might be related to differences in sampling resolution and/or rarity of both species towards the top of their stratigraphic distribution. In other localities, the extinction of both species is recorded in the uppermost *R. cushmani* Zone (Blake Nose: Huber et al. 1999; Austria: Gebhardt et al. 2010; Switzerland: Westermann et al. 2010), with the exception of an apparently earlier HO of *Th. deeckei* in Tunisia (Robaszynski et al. 1993) and Japan (Hasegawa 1999) and of *Th. greenhornensis* in Morocco (Keller et al. 2008). It is worth mentioning that different *Th. deeckei* species concepts might have been applied in the literature. For instance, Pessagno (1967) retained *Th. deeckei* as a possible junior synonym of *Th. greenhornensis*, while it has been identified as a distinct species by subsequent authors (e. g., Robaszynski et al. 1979, Ando and Huber 2007).

3) The extinction of "*G.*" *bentonensis* is recorded either below (Pueblo, Eastbourne and Clot Chevalier) or immediately above peak B on the $\delta^{13}C$ curve (Tarfaya). Because this species was not identified at wadi Bahloul and Gongzha, its extinction level in the eastern Tethyan realm cannot be assessed. Based on the available data and pending further biostratigraphic studies in sections belonging to this paleogeographic area, the HO of "*G.*" *bentonensis* appears to be a very reliable marker for the latest Cenomanian. Its apparently slightly delayed extinction in core S57 should be verified by further studies, but it is probably related to the same causes that controlled the position of the HO of *R. cushmani* (see discussion in paragraph 6.3.1). Further support to the validity of this event is provided by its consistent identification some centimeters to a few meters above the extinction of *R. cushmani* in Spain (Lamolda et al. 1997) and Morocco (Keller et al. 2008), while the apparently synchronous extinction of the single-keeled rotaliporids and of "*G.*" *bentonensis* in several Italian sections (Bottaccione-Contessa: Premoli Silva and Sliter 1995, Coccioni and Premoli Silva 2015; Antruiles, Dolomites: Luciani and Cobianchi 1999; Calabianca-Guidaloca: Scopelliti et al. 2004; Valdagno: Coccioni and Luciani 2005) is due to the absence of planktonic foraminifera in the C_{org}-enriched layers of the Bonarelli Level (or equivalent) and/or to the stratigraphic gap across the C/T boundary (Gambacorta et al. 2015).

In addition, the LOs of *D. hagni* and *D. imbricata* that are usually recognized below the beginning of the $\delta^{13}C$ isotopic excursion, also appear to be reliable for correlation as discussed below (Figs. 9–10):

4) The LO of *D. hagni* is recorded from the base of the sections in most of the localities examined, with the exception of Pont d'Issole (i.e., across the $\delta^{13}C$ rise below A) and wadi Bahloul (i.e., slightly above B). However, its appearance level is well documented in the mid-to-upper *R. cushmani* Zone at other geographic localities including Tunisia (Robaszynski et al. 1993), Morocco (Keller et al. 2008), Italy (Premoli Silva and Sliter 1995, Luciani and Cobianchi 1999, Mort et al. 2007, Coccioni and Premoli Silva 2015), Spain (Lamolda et al. 1997), Austria (Gebhardt et al. 2010), Switzerland (Westermann et al. 2010), Blake Nose (Huber et al. 1999), and Japan (Hasegawa 1999). We believe that its delayed occurrence at Pont d'Issole and wadi Bahloul might be an artifact of its rarity in these

localities and/or small-sized samples. This latter hypothesis is supported by the fact that planktonic foraminifera from Pont d'Issole and wadi Bahloul were studied in thin sections from layers characterized by a particularly indurated lithology. Thin sections represent a smaller-sized sample compared to washed residues and their study reduces the likelihood of encountering rare species. Discrepancies in the LO of *D. hagni* at low latitudes are found in the WIS: at Pueblo, the LO of *D. hagni* is below the extinction level of rotaliporids (Caron et al. 2006), while in south Texas, the LO lies above the extinction level of rotaliporids (Frush and Eicher 1975, Lowery and Leckie 2017) suggesting an ecologic influence at the southern aperture of the WIS relative to sites to the north in the core of the seaway (recorded as *P. difformis*, Eicher and Worstell 1970, Eicher and Diner 1985), indicating that the LO of this species is likely diachronous for sections within the WIS. This diachronous pattern in the WIS is similar to that of the HO of *R. cushmani*, which is also from south to north (Leckie 1985).

5) The LO of *D. imbricata* is identified from the base of the sections or in the lowermost samples at Pueblo, Eastbourne, Tarfaya, and Clot Chevalier. Its LO appears to be delayed in the sections that have been partially studied in thin section as follows: at Pont d'Issole (at excursion A), at Gongzha (slightly above excursion B), and at wadi Bahloul (in between B and C). In sections elsewhere, its LO is documented in the *R. cushmani* Zone (Italy: Premoli Silva and Sliter 1995, Luciani and Cobianchi 1999, Coccioni and Luciani 2004, Mort et al. 2007, Coccioni and Premoli Silva 2015, Spain: Lamolda et al. 1997, Japan: Hasegawa 1999, Morocco: Keller et al. 2008) and in the *W. archaeocretacea* Zone (Austria: Gebhardt et al. 2010, Switzerland: Westermann et al. 2010). Despite some discrepancies in the LO of *D. imbricata* might be related to subjective species concepts, we believe that its apparent diachronism might be an artifact of the sample size, as this species is often uncommon at the beginning of its stratigraphic range. Overall, in our opinion the appearance of *D. imbricata* can be considered a reliable bioevent for correlation in cases where the size of the samples studied is large enough to encounter rare species.

6.4.2 Potentially useful bioevents that require further investigation

1) The LO of *P. algeriana* is an upper Cenomanian event falling in the mid-upper *R. cushmani* Zone below the $\delta^{13}C$ isotope excursion A (Pueblo, Pont d'Issole, wadi Bahloul), whereas the occurrence of this species is recorded at Eastbourne, Tarfaya, Clot Chevalier and Gongzha from the base of the section, so that its LO cannot be precisely determined (Fig. 9). However, the appearance of *P. algeriana* is documented in the lower *R. cushmani* Zone (Italy: Premoli Silva and Sliter 1995, Luciani and Cobianchi 1999, Spain: Lamolda et al. 1997, Blake Nose: Huber et al. 1999). Accordingly, several authors identified a *P. algeriana* Subzone defined as the stratigraphic interval between the LO of *P. algeriana* and the HO of *R. cushmani* (Bottaccione-Contessa: Premoli Silva and Sliter 1995, Coccioni and Premoli Silva 2015, Eastbourne: Keller et al. 2001). This diachronous appearance likely reflects different species concepts among authors as testified by its accommodation either in the genus *Praeglobotruncana* (Caron 1966) or *Dicarinella* (Robaszynski et al. 1979). Recently, its distinctive morphological features have been clarified to promote its identification and calibrate its appearance level at a regional to global scale (see Falzoni et al. 2016b).

2) The occurrence of *P. oraviensis* is rarely recorded in the literature with few exceptions (Tunisia: Robaszynski et al. 1990; Spain: Lamolda et al. 1997; Crimea: Kopaevich and Vishnevskaya 2016; Clot Chevalier: Falzoni et al. 2016b) and its species concept has been differently interpreted by authors including its generic attribution, because of the unavailability of SEM images of the type material (see Falzoni et al. 2016b for taxonomic details). Possibly because of these taxonomic uncertainties, the appearance of *P. oraviensis* is recorded in different levels within the *W. archaeocretacea* Zone (Robaszynski et al. 1990, Lamolda et al. 1997, Kopaevich and Vishnevskaya 2016, Falzoni et al. 2016b). At Eastbourne, we identify the LO of *P. oraviensis* at the top of *R. cushmani* Zone, representing the oldest record of this species documented in the literature (Figs. 9–10). The delayed occurrence of *P. oraviensis* at Clot Chevalier, in the middle-upper *W. archaeocretacea* Zone likely results from a combination of sedimentologic (hiatus and condensed stratigraphic interval at the top of the *R. cushmani* Zone) and ecologically-related (very rare occurrence of planktonic foraminifera within the lower *W. archaeocretacea* Zone) causes. *Praeglobotruncana oraviensis* does not occur at Tarfaya or at Pueblo, suggesting that some ecologic features (e.g., water depth, trophic regime) might have controlled its geographic distribution at least at the beginning of its stratigraphic range, therefore the reliability of its LO requires further investigation and calibration with other sections.

3) The LO of *M. schneegansi* is recorded slightly above peak C at Pont d'Issole (Grosheny et al. 2006), while ancestral morphotypes named *M.* cf. *schneegansi* do occur at Clot Chevalier approximately in the same stratigraphic interval (Falzoni et al. 2016b) (Fig. 9). The LO of *M. schneegansi* is identified in sediments of approximately coeval age either slightly below (Japan: Hasegawa 1999) or above the LO of *H. helvetica* (Tunisia: Robaszynski et al. 1990; Italy: Premoli Silva and Sliter 1995, Coccioni and Premoli Silva 2015; Texas: Lowery and Leckie 2017). Unfortunately, the synchronicity of the appearance of *M. schneegansi* in these sections cannot be accurately tested in the absence of a $\delta^{13}C$ profile. In addition, *M. schneegansi* is not documented in the lowermost Turonian of the other localities examined and it is absent in the southern mid- to high latitudes (Petrizzo 2000, 2001), suggesting that its geographic distribution might be confined to the tropical-subtropical latitudinal belt. Consequently, the reliability of its LO requires further study, but it might represent a useful bioevent falling close to the C/T boundary at least at low latitudes (Fig. 10).

4) The LO of *M. sigali* is detected well above peak C, but within the *H. helvetica* Zone, at Pueblo and at Gongzha, although it seems to be delayed in the former section. Possible ancestral morphotypes of *M. sigali* occur at Clot Chevalier approximately across the same stratigraphic interval (above C) (Fig. 9). This species is absent at Tarfaya, Eastbourne, Pont d'Issole, and wadi Bahloul, but it is usually documented to first occur slightly below (Furlo: Mort et al. 2007; south Texas: Lowery and Leckie 2017), or above the LO of *H. helvetica* (Tunisia: Robaszynski et al. 1990; Italy: Premoli Silva and Sliter 1995, Coccioni and Premoli Silva 2015; Switzerland: Westermann et al. 2010; Tanzania: Huber et al. 2017). Because the appearance level of *M. sigali* is still not documented in several localities, its reliability for low to mid-latitude correlation requires further investigation.

5) LO of other *Marginotruncana* species. The LO of *M. renzi* was identified well above C at the top of the Eastbourne section by Paul et al. (1999) in a slightly younger stratigraphic interval compared to that here re-studied and assigned to the ammonite *Mammites nodosoides* Zone (Figs. 3 and 9). The LO of *M. renzi* is documented slightly above the LO of *H. helvetica* at Blake Nose (Huber et al. 1999), in south Texas (Lowery and Leckie 2017), Italy (Premoli Silva and Sliter 1995, Coccioni and Premoli Silva 2015), and Tunisia (Robaszynski et al. 1990). The LO of *M. marianosi* is documented at Pueblo falling in the *H. helvetica* Zone and above peak C, where the $\delta^{13}C$ returns close to pre-excursion values (Fig. 9). In other localities, the LO of *M. marianosi* is recorded below (Furlo: Mort et al. 2007) or slightly above (Bottaccione-Contessa: Premoli Silva and Sliter 1995) the LO of *H. helvetica*, but this bioevent is significantly delayed in the southern mid-latitudes (Exmouth Plateau: Petrizzo 2000), as it falls above the extinction of *Falsotruncana maslakovae* in the late Turonian – early Coniacian. The LO of *M. coronata* is identified in the lower (Pont d'Issole: Grosheny et al. 2006) or at the top of the *H. helvetica* Zone in the Tethyan Realm (Tunisia: Robaszynski et al. 1990; Italy: Premoli Silva and Sliter 1995, Coccioni and Premoli Silva 2015; Tanzania: Huber and Petrizzo 2014, Huber et al. 2017), and in the southern mid-latitudes (Exmouth Plateau: Petrizzo 2000). In south Texas, the LO of *M. coronata* is above the HO of *H. helvetica* (Frush and Eicher 1975, Lowery and Leckie 2017).

Overall, the reliability for correlation of *Marginotruncana* species needs further investigation and calibration with the carbon isotope record at other localities. It is noteworthy that the appearance of marginotruncanids predates the LO of *H. helvetica* in the southern Indian Ocean (Kerguelen Plateau: Petrizzo 2001), potentially representing a valuable event for correlating low-to-high latitude records and for approximating the C/T boundary at high latitudes, where the more thermophilic *H. helvetica* is absent.

6.4.3 Misleading bioevents

1) The LO of *H. praehelvetica* has been recorded in different stratigraphic intervals from below peak A to below peak B (Fig. 9). Specimens strictly resembling the holotype of *H. praehelvetica* were not identified at Eastbourne during this study, while we recognized the LO of possibly primitive and poorly developed specimens that may be phylogenetically related to this species and here named *H.* cf. *praehelvetica* below the beginning of the $\delta^{13}C$ isotopic excursion (Fig. 9). The LO of *H. praehelvetica* is documented in previous works at Eastbourne (Paul et al. 1999, Keller et al. 2001, Hart et al. 2002) (Fig. 3), but the absence of figured *H. praehelvetica* specimens in these papers prevents a comparison of the species concepts adopted. On the other hand, the combined absence of the true *H. praehelvetica* and of its descendant *H. helvetica* might suggest adverse ecological conditions for both species at Eastbourne. In other sections, this bioevent is identified either in the *R. cushmani* Zone (Bottac-

cione: Premoli Silva and Sliter 1995; Furlo: Mort et al. 2007; Antruiles, Dolomites: Luciani and Cobianchi 1999; Blake Nose: Huber et al. 1999; Tarfaya: Keller et al. 2008), at the extinction level of the rotaliporids (Leckie 1985, Falzoni et al. 2016b), or within the lower *W. archaeocretacea* Zone (Tunisia: Robaszynski et al. 1990; Spain: Lamolda et al. 1997). These discrepancies are likely due to the common occurrence of transitional morphotypes between *H. praehelvetica* and its ancestor *Whiteinella aprica* making the identification of the first representative of the species subjective (Huber and Petrizzo 2014). Accordingly, the occurrence of *W. aprica* is recognized from the base of the sections and below the LO of *H. praehelvetica* at Tarfaya (core S57) and in several other localities (see Leckie 1985, Lamolda et al. 1997, Luciani and Cobianchi 1999, Keller et al. 2008, Falzoni et al. 2016b). By contrast, the occurrence of *W. aprica* is not documented in other sections where only the higher spired *W. brittonensis* is observed below and above the LO of *H. praehelvetica*. A possible explanation to this contradiction is the general rarity of *W. aprica* in the late Cenomanian as opposed to the occurrence of abundant intermediate morphotypes between *W. aprica* and *W. brittonensis* (as we observed at Eastbourne and Tarfaya) that some authors might have included in the range of variability of the latter species. Because of the observations listed above, we regard the LO of *H. praehelvetica* as an unreliable marker for correlation.

2) *Whiteinella archaeocretacea* occurs from the base (or nearly the base) of the section at Pueblo, Eastbourne, Gongzha and wadi Bahloul, while its LO is recorded slightly below A at Pont d'Issole. Specimens strictly resembling the holotype were not identified at Tarfaya and Clot Chevalier (Fig. 9). At Eastbourne, *W. archaeocretacea* is extremely rare and it shows a very discontinuous stratigraphic distribution, suggesting that the identification of its lowest appearance level might be strongly biased by a low sampling resolution or by the analyses of small-sized samples. Discrepancies in its LO might also be due to a subjective species concept, because specimens having a rounded (resembling the holotype) as well as a pinched lateral profile (resembling the paratype) were retained to fall in its range of variability. Pending further taxonomic studies and because of its rarity in the assemblages, we regard the LO of *W. archaeocretacea* as an unreliable bioevent.

3) The extinctions of *R. montsalvensis* and *Th. brotzeni* have been identified at Gongzha well below the $\delta^{13}C$ excursion. At Eastbourne *Th. brotzeni* disappears in the stratigraphic interval where we observe the first $\delta^{13}C$ rise, while *R. montsalvensis* becomes extinct slightly above the beginning of the second $\delta^{13}C$ rise, both below peak A (Figs. 3 and 9). Both bioevents have been recorded to fall in the middle *R. cushmani* Zone in the Bottaccione-Contessa composite section (Coccioni and Premoli Silva 2015), where *R. montsalvensis* and *Th. brotzeni* show a scattered occurrence toward the top of their stratigraphic range (as well as at Eastbourne), leading to some uncertainties regarding the position of their extinction level. By contrast, other studies indicate that the HO of both species falls in an older stratigraphic interval below the appearance of *R. cushmani* (Hasegawa 1999, Westermann et al. 2010). Pending further studies, we interpret the HO of *R. montsalvensis* and *Th. brotzeni* as being controlled by local environmental conditions and because of their rarity toward the top of their stratigraphic distribution we discourage using their extinction level for correlation.

4) The LO of *D. elata* is recorded below excursion A (Pueblo, Clot Chevalier, Eastbourne) and above excursion B (wadi Bahloul and Gongzha) (Fig. 9). Remarkably, *D. elata* is identified as co-occuring with *Thalmanninella globotruncanoides* in the middle Cenomanian of Tunisia (Kalaat Senan: Robaszynski et al. 1993), representing its oldest documented record in the literature. Most studies identified its LO in the uppermost *R. cushmani* Zone in Spain (Lamolda et al. 1997), whereas its occurrence is not recognized at Tarfaya and Pont d'Issole, in the Italian sections (Bottaccione section: Premoli Silva and Sliter 1995, Coccioni and Luciani 2004, Coccioni and Premoli Silva 2015; Antruiles, Dolomites: Luciani and Cobianchi 1999; Furlo: Mort et al. 2007), at Blake Nose (Huber et al. 1999), in Morocco (Keller et a. 2008), Switzerland (Westermann et al. 2010) and Japan (Hasegawa 1999). Although discrepancies in its LO might be related to the rarity of *D. elata* in some environmental settings, and considering that its occurrence might not be detected in small-sized samples and poorly resolved biostratigraphic studies, the observations listed above support its unreliability for correlation because of its presumably stenotopic ecology and absence in several localities. Discrepancies in the identification of its appearance level may also relay on different species concepts.

5) The LO of *D. canaliculata* has been recorded to fall in different stratigraphic levels as follows: below the initial $\delta^{13}C$ positive excursion (Pueblo and Eastbourne), slightly below excursion A (Clot Chevalier),

and above excursion C (Pont d'Issole and wadi Bahloul), while it is absent at Tarfaya and Gongzha (Fig. 9). Discrepancies in its appearance level are found in other localities: its LO is identified in the upper *R. cushmani* Zone (Bottaccione-Contessa: Coccioni and Premoli Silva 2015; Antruiles, Dolomites: Luciani and Cobianchi 1999; Japan: Hasegawa 1999), within the *W. archaeocretacea* Zone (Blake Nose: Huber et al. 1999), and within the *H. helvetica* Zone (Tunisia: Robaszynski et al. 1990). The sections in south Texas may have experienced conditions of environmental exclusion, very low abundances, and/or poor preservation that result in a much delayed LO of *D. canaliculata* within or at the top of the *H. helvetica* Zone (Lowery and Leckie 2017). Based on the above and on its distinctive morphology, we interpret this bioevent to be considerably diachronous and likely subject to ecological control.

6) The genus *Anaticinella* was erected to include ecophenotypes that evolved from the typical single-keeled rotaliporids by losing the peripheral keel and inflating the chambers on both the umbilical and spiral sides (Eicher 1973); this morphologic adaptation was interpreted as forced by the expansion of the oxygen minimum zone at the onset of OAE 2 that induced the exploitation of sea-surface habitats by taxa that were deep-dwellers (Wonders 1980, Leckie 1985, Desmares et al. 2007). Two species were included in the genus *Anaticinella* (= *Pseudoticinella* Longoria 1973): *multiloculata* and *planoconvexa* (Longoria 1973). More recently, *planoconvexa* was accommodated in the genus *Rotalipora*, as it was interpreted to directly evolve from *R. cushmani* (Desmares et al. 2008), while the species *multiloculata* belongs to the *Th. greenhornensis* phyletic lineage, and thus has been accommodated in the genus *Thalmanninella* (González-Donoso et al. 2007, Desmares et al. 2008). *Anaticinella* species have been largely documented in the WIS (Morrow 1934, Eicher and Worstell 1970, Eicher 1973, Leckie 1985, Keller and Pardo 2004, Caron et al. 2006, Desmares et al. 2007, 2008), but their occurrence is also recorded in other low latitude localities (Eastbourne: Keller et al. 2001; France: Grosheny et al. 2006; Tunisia: Caron et al. 2006; Grosheny et al. 2013; Morocco: Keller et al. 2008; Tibet: Bomou et al. 2013).

Desmares et al. (2007) identified the extinction of *Th. multiloculata* and *R. planoconvexa* at Pueblo as follows: a) HO *Th. multiloculata* slightly above excursion A, and b) HO *R. planoconvexa* slightly above excursion C (Fig. 9). The HO of *Th. multiloculata* is recorded below peak A at Pont d'Issole (Grosheny et al. 2006), while the HO of *Anaticinella* species is recorded above peak A at Gongzha (Bomou et al. 2013) and slightly above peak C at wadi Bahloul (Caron et al. 2006). Morphotypes falling in the range of variability of *Th. multiloculata* and *R. planoconvexa* are not identified at Clot Chevalier (Falzoni et al. 2016b) and neither at Eastbourne and Tarfaya, although *Th. multiloculata* is recognized at Eastbourne by Keller et al. (2001). Specimens resembling *R. cushmani* but having 4 to 5 more inflated chambers and a very weakly developed peripheral keel on the first chambers of the last whorl occur rarely at Eastbourne (here figured in Fig. 5, 2a–c). In our opinion and according to Robaszynski et al. (1993), these specimens closely resemble the original description and the drawing of the holotype of *Rotalipora praemontsalvensis* (Ion 1976), rather than *R. planoconvexa* (Longoria 1973). They also resemble specimens identified as *R. cushmani* Morphotype 1 in the Tarfaya Basin and supposed to share some morphological similarities to the anaticinellids endemic of the WIS (Luderer and Kuhnt 1997). However, we believe that these specimens differ from the typical anaticinellids of the WIS because of the smoother wall texture and the lower number of chambers in the last whorl that are semicircular rather than subrectangular on the spiral side. However, such specimens might have been included in the genus *Anaticinella* or in the atypical *R. cushmani* morphotypes by previous authors (e. g., Leckie 1985, Caron et al. 2006, Desmares et al. 2007), especially when observed in thin sections. Further studies are required to better assess the taxonomic status and phyletic relationship among rotaliporids. On the other hand, the geographic distribution of *Th. multiloculata* and of *R. planoconvexa* (sensu stricto) should be further investigated and their occurrence outside the WIS should be more robustly supported. However, the extinction of *Anaticinella* species is clearly diachronous (Fig. 9).

7) The "*Heterohelix*" shift was first identified by Leckie (1985), Leckie et al. (1998), and West et al. (1998) in the WIS as an abrupt change in planktonic foraminiferal assemblages, which became dominated by the biserial species *moremani* and *globulosa* at that time included in the genus *Heterohelix* and recently accommodated in the genus *Planoheterohelix* (Haynes et al. 2015). This change in the composition of the assemblages has been interpreted as an ecologic event resulting from a period of unstable eutrophic surface water conditions that inhibited the proliferation of the keeled K-strategist taxa. However, no precise definition of "*Heterohelix*" shift was given at the time of its

first identification in the WIS, although relative abundances of biserials within this shift were on average higher than 50 % in the > 63 μm size fraction. Over the years, the term "*Heterohelix*" shift has been generically used to identify a major increase in the abundance of biserial taxa across the C–T boundary interval, without any constrains regarding the species contributing to the shift, the size fractions studied and the threshold value of relative abundances yielded by biserials for defining the onset of the event. For instance, the "*Heterohelix*" shift was sometimes recognized based on thin section studies, thus including the < 63 μm population (Caron et al. 2006, Bomou et al. 2013), while biserial species other than *moremani* and *globulosa* are documented to contribute to the "*Heterohelix*" shift across the C–T boundary interval (*Planoheterohelix reussi*: Keller et al. 2001; *Laeviheterohelix pulchra*: Caron et al. 2006; *Planoheterohelix paraglobulosa*: this study). Moreover, the relative abundance of biserial taxa and the size fractions studied are sometimes not specified or are different from those reported by Leckie (1985) and Leckie et al. (1998). While we believe that all biserial species (not only *moremani* and *globulosa*) that increase in abundance across the C–T boundary interval have to be considered for the identification of the "*Heterohelix*" shift, we underline that a more objective identification of this event in washed residues should strictly follow the criteria applied by Leckie (1985) and Leckie et al. (1998) to include the relative abundance of all biserials (> 50 % of the planktonic foraminiferal assemblage) and size fraction (> 63 μm). Here we suggest to arbitrarily place the onset of the "*Heterohelix*" shift at the lowermost sample in which biserials are equal to or exceed the 50 % of the planktonic foraminiferal assemblage, as first described by Leckie et al. (1998). On the other hand, this approach does not ensure an objective identification of the "*Heterohelix*" shift in thin section studies. In fact, Nederbragt and Fiorentino (1999) demonstrated that there is a quite significant offset in the stratigraphic position at which the onset of the "*Heterohelix*" shift would be placed in Tunisia, when identified on the > 63 μm size fraction or on thin sections.

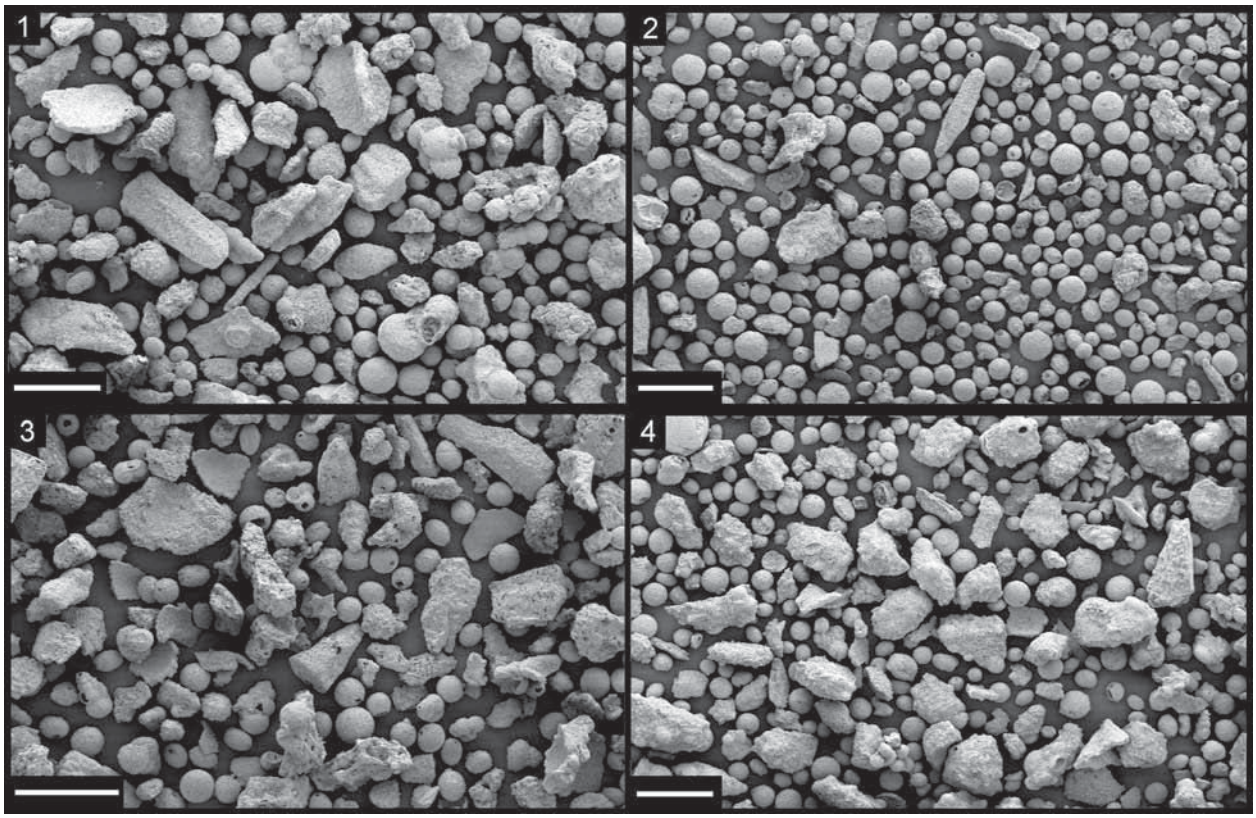

Fig. 11. SEM images of the washed residues obtained from the rock samples collected at Eastbourne showing the composition of the assemblage in the < 125 μm size-fraction with dominant calcispheres and rare biserial taxa. 1) Sample WC300 (16.9 m); 2) sample WC500 (18.9 m); 3) sample WC800 (21.9 m); and 4) sample WC1300 (26.9 m). Scale bar = 200 μm.

A different approach for defining the "*Heterohelix*" shift is also applied in the sections considered in this study. Keller et al (2001) identified the "*Heterohelix*" shift near peak B based on the increase in abundance from 20 to over 60 % of the species *moremani* and *reussi* in the >63 µm size fraction at Eastbourne. Such a dominance of heterohelicids could not be confirmed in the samples examined during this study that instead revealed an increase in the abundance of calcispheres in the same stratigraphic interval (Fig. 11), as reported by Pearce et al. (2009). By contrast, we observed a marked increase in the abundance of biserial taxa (species *moremani*, *paraglobulosa*, *globulosa*) in core S57 (Tarfaya). The onset of the "*Heterohelix*" shift is here placed according to Leckie (1985) and Leckie et al. (1998) at the lowermost sample yielding biserials representing more than the 50 % of the assemblage in the >63 µm size fraction and lies slightly above peak B. At wadi Bahloul, the "*Heterohelix*" shift is identified between excursions A and B based on the marked increase in the abundance of the species *moremani*, *globulosa* and of *Laeviheterohelix pulchra* in washed residues (>38 µm) and in thin section samples, while at Gongzha the abundance of biserial taxa increased below excursion A based on the observation of thin sections, but the species occurring in that stratigraphic interval were not specified (Fig. 9). The "*Heterohelix*" shift is not documented in the Vocontian Basin (Clot Chevalier: Falzoni et al. 2016b, Pont d'Issole: Grosheny et al. 2006), but it is recognized in the lower-middle *W. archaeocretacea* Zone of other localities (Italy: Coccioni and Luciani 2004; Tunisia: Nederbragt and Fiorentino 1999; Morocco: Keller et al. 2008), with the exception of Huber et al. (1999), who identified this bioevent in the lowermost *H. helvetica* Zone, thus in the early Turonian, at Blake Nose. The increase in the abundance of biserial taxa recently documented in Tanzania (Haynes et al. 2015, Huber et al. 2017) falls well above the extinction of *H. helvetica* in a much younger stratigraphic interval assigned to the late Turonian *M. sinuosa–H. huberi* Zone. This latter event named "Biserial shift" (Huber et al. 2017) is surely not related to the "*Heterohelix*" shift of the C–T boundary interval, because of the stratigraphic gap separating the two events.

The onset of the "*Heterohelix*" shift across the Cenomanian–Turonian boundary interval is only slightly diachronous at Pueblo and Tarfaya (Fig. 8b), nevertheless inconsistencies in the definition of the "*Heterohelix*" shift applied in the literature and its close relation to the ecologic features of sea-surface waters discourage its application for interbasinal correlations.

7. Conclusions

A highly-resolved biostratigraphic analysis of planktonic foraminiferal assemblages at Eastbourne (UK) and Tarfaya (Morocco), compared with the record at the Turonian GSSP in Colorado, allowed recognition of a sequence of bioevents that are compared to those recorded in other sections available in the literature and correlated to the $\delta^{13}C$ profile. We calculated reliable estimates of the age of most planktonic foraminiferal events identified in the Pueblo GSSP section, including the extinction of *R. cushmani* and the appearance of *H. helvetica*. Results of graphic correlations and comparison between the sections analyzed indicate that the extinctions of Cenomanian taxa represent the most reproducible sequence of bioevents at low to mid-latitudes and should be considered reliable for supra-basinal correlations. This sequence includes, in stratigraphic order, the HOs of: (1) *Th. deeckei*, (2) *Th. greenhornensis*, (3) *R. cushmani*, and (4) "*G.*" *bentonensis*. The LOs of *D. hagni* and *D. imbricata* in the pre-excursion interval may be considered as additional reliable bioevents for correlation in case the size of samples used for planktonic foraminiferal biostratigraphy is large enough to ensure the identification of rare species.

Additional useful bioevents that, however, require further investigation, because of their rare identification in several localities or poor calibration with other bio- and chemostratigraphic data include the LOs of *P. oraviensis* at the top of the *R. cushmani* Zone and *M. schneegansi*, the latter being particularly promising to approximate the C/T boundary in low latitude localities. Little information is presently available to test the synchronicity of the appearance of *P. algeriana* in the mid-upper Cenomanian and of other *Marginotruncana* species (i.e., *M. sigali*, *M. renzi*, *M. coronata* and *M. marianosi*) in the Turonian, but these events appear worthy of further investigation. By contrast, the geographic and stratigraphic distribution of *D. elata*, and *D. canaliculata* were likely ecologically driven. Inconsistencies in the application of different species concepts by authors are difficult to assess, but they might have introduced additional discrepancies in the identification of their LOs. A highly transitional evolution from the ancestral species, rarity and different species concepts among authors can be invoked as a cause for the diachronous LOs of *H. praehelvetica* and *H. helvetica*, while *W. archaeocretacea*, *Th. brotzeni* and *R. montsalvensis* occur too rarely in the stratigraphic interval examined, so that their appearance/extinction can be misleading to trace correlations. Finally, our

study confirms the unreliability of the LO of *H. helvetica* as a marker for the base of the Turonian and suggests that the "*Heterohelix*" shift, here precisely defined in order to ensure a more objective identification, represents a response of the planktonic foraminiferal assemblages to a local/regional increase in sea-surface productivity, salinity, or temperatures. In addition, we highlight that the occurrence of anaticinellids (sensu strictu) is still poorly documented outside the WIS and, regardless, their extinctions are clearly diachronous.

To conclude, we suggest that further efforts need to be directed toward the stabilization of the taxonomic concepts of several planktonic foraminiferal species in order to assure an univocal approach during biostratigraphic analyses. Moreover, a small sample size and/or a low sampling resolution might significantly influence the level at which LOs and HOs are identified even when the bioevent is geologically isochronous. These factors should be taken in consideration when establishing correlations. On the other hand, we emphasize that identification of the $\delta^{13}C$ peaks and troughs is not straightforward and should always be supported by a highly-resolved sequence of bioevents.

Acknowledgements. We are indebted to the editor Jochen Erbacher, and to Wolfgang Kuhnt and Brian T. Huber for their thoughtful reviews that greatly improved the quality of this manuscript. Agostino Rizzi (CNR, Italy) is thanked for assistance at the SEM. FF carried out this research during a post-doc fellowship of the University of Milan. This study was funded by MIUR-PRIN 2010–2011 (2010X3PP8J_001) to Elisabetta Erba (scientific coordinator).

References

Ando, A., Huber, B.T., 2007. Taxonomic revision of the late Cenomanian planktonic foraminifera *Rotalipora greenhornensis* (Morrow, 1934). Journal of Foraminiferal Research 37, 160–174.

Anthonissen, D.E., Ogg, J.G., 2012. Appendix 3: Cenozoic and Cretaceous biochronology of planktonic foraminifera and calcareous nannofossils. The Geologic Time Scale 2012, 1083–1127.

Arthur, M.A., Dean, W.E., Pollastro, R., Scholle, P.A., Claypool, G.E., 1985. A comparative geochemical study of two transgression pelagic limestone units, Cretaceous Western Interior basin, U.S. In: Pratt, L.A., Kauffman, E.G., Zelt, F.B. (Eds.), Fine Grained Deposits and Biofacies of the Cretaceous Western Interior Seaway: evidence of cyclic sedimentary processes. Field Trip Guidebook, vol.4. Society of Economic Paleontologists and Mineralogists, Tulsa, pp. 16–27.

Arthur, M.A., Schlanger, S.O., Jenkyns, H.C., 1987. The Cenomanian-Turonian oceanic anoxic event II. Paleoceanographic controls on organic-matter production and preservation. In: Brooks, J., Fleet, A.J. (Eds.), Marine Petroleum Source Rocks. Geological Society, London, Special Publication No. 26, 401–420.

Bolli, H.M., 1945. Zur Stratigraphie der oberen Kreide in den höheren helvetischen Decken. Eclogae Geologicae Helvetiae 37, 217–328.

Bomou, B., Adatte, T., Tantawy, A.A., Mort, H., Fleitmann, D., Huang, Y., Föllmi, K.B., 2013. The expression of the Cenomanian–Turonian oceanic anoxic event in Tibet. Palaeogeography, Palaeoclimatology, Palaeoecology 369, 466–481.

Bowman, A.R., Bralower, T.J., 2005. Paleoceanographic significance of high-resolution carbon isotope records across the Cenomanian–Turonian boundary in the Western Interior and New Jersey coastal plain, USA. Marine Geology 217, 305–321.

Bralower, T.J., Leckie, R.M., Sliter, W.V., Thierstein, H.R., 1995. An integrated Cretaceous microfossil biostratigraphy. In: Berggren, W.A., Kent, D.V., Aubry, M.-P., Hardenbol, J., (Eds.), Geochronology, Time Scales, and Global Stratigraphic Correlation. Society for Sedimentary Geology, SEPM Special Publication 54, 6–579.

Caldwell, W.G.E., Kauffman, E.G., 1993. Evolution of the Western Interior basin. St. John's, Geological Association of Canada Special Papers 39, 680 pp.

Caron, M., 1966. Globotruncanidae du Crétacé supérieur du synclinal de la Gruyère (Préalpes medians, Suisse). Revue de Micropaléontologie 9, 68–93.

Caron, M., Dall'Agnolo, S., Accarie, H., Barrera, E., Kauffman, E.G., Amédro, F., Robaszynski, F., 2006. High-resolution stratigraphy of the Cenomanian–Turonian boundary interval at Pueblo (USA) and wadi Bahloul (Tunisia): Stable isotope and bio-events correlation. Géobios 39, 171–200.

Carter, D.J., Hart, M.B., 1977, Aspects of mid-Cretaceous stratigraphical micropalaeontology. Bulletin of the British Museum of Natural History, Geological Series 29, 1–135.

Cobban, W.A., Scott, G.R., 1972. Stratigraphy and ammonite fauna of the Graneros Shale and Greenhorn Limestone near Pueblo, Colorado (No. 645). United States Geological Survey Professional Paper 645, 108 pp.

Coccioni, R., Luciani, V., 2004. Planktonic foraminifera and environmental changes across the Bonarelli Event (OAE2, latest Cenomanian) in its type area: A high resolution study from the Tethyan reference Bottaccione section (Gubbio, central Italy). Journal of Foraminiferal Research 34, 109–129.

Coccioni, R., Luciani, V., 2005. Planktonic foraminifers across the Bonarelli Event (OAE2, latest Cenomanian): The Italian record. Palaeogeography, Palaeoclimatology, Palaeoecology 224, 167–185.

Coccioni, R., Premoli Silva, I., 2015. Revised Upper Albian–Maastrichtian planktonic foraminiferal biostratigraphy and magneto-stratigraphy of the classical Tethyan

Gubbio section (Italy). Newsletters on Stratigraphy 48, 47–90.

Corbett, M.J., Watkins, D.K., 2013. Calcareous nannofossil paleoecology of the mid-Cretaceous Western Interior Seaway and evidence of oligotrophic surface waters during OAE2. Palaeogeography, Palaeoclimatology, Palaeoecology 392, 510–523.

Desmares, D., Grosheny, D., Beaudoin, B., Gardin, S., Gauthier-Lafaye, F., 2007. High resolution stratigraphic record constrained by volcanic ashes layers at the Cenomanian–Turonian boundary in the Western Interior Basin, USA. Cretaceous Research 28, 561–582.

Desmares, D., Grosheny, D., Beaudoin, B., 2008. Ontogeny and phylogeny of Upper Cenomanian rotaliporids (Foraminifera). Marine Micropaleontology 69, 91–105.

Eicher, D.L., 1973. Phylogeny of the late Cenomanian planktonic foraminifer *Anaticinella multiloculata* (Morrow). Journal of Foraminiferal Research 2, 184–190.

Eicher, D.L., Diner, R., 1985. Foraminifera as indicators of water mass in the Cretaceous Greenhorn Sea, Western Interior. In: Pratt, L.M., Kauffman, E.G., Zelt, F.B. (Eds.), Fine-grained Deposits and Biofacies of the Cretaceous Western Interior Seaway: Evidence of Cyclic Sedimentary Processes, Field Trip Guidebook, Society of Economic Paleontologists and Mineralogists 4, 60–71.

Eicher, D.L., Worstell, P., 1970. Cenomanian and Turonian foraminifera from the Great Plains, United States. Micropaleontology 16, 269–324.

Elder, W.P., 1988. Geometry of Upper Cretaceous bentonite beds: Implications about volcanic source areas and paleowind patterns, Western Interior, United States. Geology 16, 835–838.

Elderbak, K., Leckie, R.M., 2016. Paleocirculation and foraminiferal assemblages of the Cenomanian–Turonian Bridge Creek Limestone bedding couplets: Productivity vs. dilution during OAE2. Cretaceous Research 60, 52–77.

Elderbak, K., Leckie, R.M., Tibert, N.E., 2014. Paleoenvironmental and paleoceanographic changes across the Cenomanian–Turonian Boundary Event (Oceanic Anoxic Event 2) as indicated by foraminiferal assemblages from the eastern margin of the Cretaceous Western Interior Sea. Palaeogeography, Palaeoclimatology, Palaeoecology 413, 29–48.

Eldrett, J.S., Ma, C., Bergman, S.C., Lutz, B., Gregory, F.J., Dodsworth, P., Phipps, M., Hardas, P., Minisini, D., Ozkan, A., Ramezani, J., Bowring, S.A., Kamo, S.L., Ferguson, K., Macaulay, C., Kelly, A.E., 2015. An astronomically calibrated stratigraphy of the Cenomanian, Turonian and earliest Coniacian from the Cretaceous Western Interior Seaway, USA: Implications for global chronostratigraphy. Cretaceous Research 56, 316–344.

Erbacher, J., Friedrich, O., Wilson, P.A., Birch, H., Mutterlose, J., 2005. Stable organic carbon isotope stratigraphy across Oceanic Anoxic Event 2 of Demerara Rise, western tropical Atlantic. Geochemistry, Geophysics, Geosystems 6, Q06010, doi:10.1029/2004GC000850.

Falzoni, F., Petrizzo, M.R., Clarke, L.J., MacLeod, K.G., Jenkyns, H.C., 2016a. Long-term Late Cretaceous oxygen- and carbon-isotope trends and planktonic foraminiferal turnover: A new record from the southern midlatitudes. Geological Society of America Bulletin 128, 1725–1735.

Falzoni, F., Petrizzo, M.R., Jenkyns, H.C., Gale, A.S., Tsikos, H., 2016b. Planktonic foraminiferal biostratigraphy and assemblage composition across the Cenomanian–Turonian boundary interval at Clot Chevalier (Vocontian Basin, SE France). Cretaceous Research 59, 69–97.

Falzoni, F., Petrizzo, M.R., MacLeod, K.G., Huber, B.T., 2013. Santonian–Campanian planktonic foraminifera from Tanzania, Shatsky Rise and Exmouth Plateau: Species depth ecology and paleoceanographic inferences. Marine Micropaleontology 103, 15–29.

Forster, A., Schouten, S., Moriya, K., Wilson, P.A., Sinninghe Damsté, J.S., 2007. Tropical warming and intermittent cooling during the Cenomanian/Turonian oceanic anoxic event 2: Sea surface temperature records from the equatorial Atlantic. Paleoceanography 22, PA1219, doi:10.1029/2006PA001349.

Frush, M.P., Eicher, D.L., 1975. Cenomanian and Turonian foraminifera and paleoenvironments in the Big Bend region of Texas and Mexico. In: Caldwell, W.G.E. (ed.), The Cretaceous System in the Western Interior of North America: The Geological Society of Canada Special Paper 13, p.277–301.

Gale, A.S., Christensen, W.K., 1996. Occurrence of the belemnite *Actinocamax plenus* in the Cenomanian of SE France and its significance. Bulletin of the Geological Society of Denmark 43, 68–77.

Gale, A.S., Kennedy, W.J., Voigt, S., Walaszczyk, I., 2005. Stratigraphy of the Upper Cenomanian–Lower Turonian Chalk succession at Eastbourne, Sussex, UK: Ammonites, inoceramid bivalves and stable carbon isotopes. Cretaceous Research 26, 460–487.

Gambacorta, G., Jenkyns, H.C., Russo, F., Tsikos, H., Wilson, P.A., Faucher, G., Erba, E., 2015. Carbon- and oxygen-isotope records of mid-Cretaceous Tethyan pelagic sequences from the Umbria–Marche and Belluno Basins (Italy). Newsletters on Stratigraphy 48, 299–323.

Gebhardt, H., Friedrich, O., Schenk, B., Fox, L., Hart, M.B., and Wagreich, M., 2010. Paleoceanographic changes at the northern Tethyan margin during the Cenomanian–Turonian Oceanic Anoxic Event (OAE-2): Marine Micropaleontology 77, 25–45.

Georgescu, M.D., 2007. A new planktonic heterohelicid foraminiferal genus from the Upper Cretaceous (Turonian). Micropaleontology 53, 212–220.

Georgescu, M.D., Huber, B.T., 2009. Early evolution of the Cretaceous serial planktic foraminifera (late Albian–Cenomanian). Journal of Foraminiferal Research 39, 335–360.

González-Donoso, J.M., Linares, D., Robaszynski, F., 2007. The rotaliporids, a polyphyletic group of Albian–Cenomanian planktonic foraminifera: Emendation of genera. Journal of Foraminiferal Research 37, 175–186.

Gradstein, F.M., Ogg, J.G., Schmitz, M.D., Ogg, G.M., 2012. The Geologic Time Scale 2012. Oxford, UK, Elsevier, 1144 p.

Grosheny, D., Beaudoin, B., Morel, L., Desmares, D., 2006. High-resolution biostratigraphy and chemostratigraphy of the Cenomanian–Turonian Boundary Event in the Vocontian Basin, S-E France. Cretaceous Research 27, 629–640.

Grosheny, D., Ferry, S., Jati, M., Ouaja, M., Bensalah, M., Atrops, F., Chikhi-Aouimeur, F., Benkerouf-Kechid, F., Negra, H., Salem, H.A., 2013. The Cenomanian–Turonian boundary on the Saharan Platform (Tunisia and Algeria). Cretaceous Research 42, 66–84.

Grosheny, D., Ferry, S., Lecuyer, C., Thomas, A., Desmares, D., 2017. The Cenomanian–Turonian Boundary Event (CTBE) on the southern slope of the Subalpine Basin (SE France) and its bearing on a probable tectonic pulse on a larger scale. Cretaceous Research, 72, 39–65.

Hart, M.B., Carter, D.J., 1975. Some observations on the Cretaceous Foraminiferida of southeast England: Journal of Foraminiferal Research 5, 114–126.

Hart, M.B., 1999. The evolution and biodiversity of Cretaceous planktonic Foraminiferida. Geobios 32, 247–255.

Hart, M.B., 2008. Cretaceous foraminifera from the Turonian succession at Beer, southeastern Devon, England. Cretaceous Research 29, 1035–1046.

Hart, M.B., Bigg, P.J., 1981. Anoxic events in the Late Cretaceous chalk seas of NW Europe. In: Neale, J.W., Brasier, M.D. (Eds.), Microfossils of Recent and Fossil Shelf Seas: Ellis Horwood Ltd., Chichester, 177–185.

Hart, M.B., Monteiro, J.F., Watkinson, M.P., Price, G.D., 2002. Correlation of events at the Cenomanian/Turonian boundary: Evidence from Southern England and Colorado. In: Wagreich, M. (Ed.), Aspects of Cretaceous Stratigraphy and Palaeobiogeography. Schriftenreihe der erdwissenschaftliche Kommission der Österreichische Akademie der Wissenschaften, Wien, 15: 35–46, Verlag der Österreichische Akademie der Wissenschaften, Wien.

Hart, M.B., Weaver, P.P.E., 1977. Turonian microbiostratigraphy of Beer, SE Devon: Proceedings of the Ussher Society 4, 86–93.

Hasegawa, T., 1999. Planktonic foraminifera and biochronology of the Cenomanian-Turonian (Cretaceous) sequence in the Oyubari area, Hokkaido, Japan. Paleontological Research 3, 173–192.

Hay, W.W., DeConto, R., Wold, C.N., Wilson, K.M., Voigt, S., Schulz, M., Wold-Rossby, A., Dullo, W.C., Ronov, A.B., Balukhovsky, A.N., Soeding, E., 1999. Alternative global Cretaceous paleogeography. In: Barrera, E., Johnson, C.C. (Eds.), The Evolution of the Cretaceous Ocean/Climate System. Special Papers of the Geological Society of America 332, 1–47.

Haynes, S.J., Huber, B.T., MacLeod, K.G., 2015. Evolution and phylogeny of mid-Cretaceous (Albian–Coniacian) biserial planktic foraminifera. Journal of Foraminiferal Research 45, 42–81.

Hilbrecht, H., Arthur, M.A., Schlanger, S.O., 1986. The Cenomanian–Turonian boundary event; sedimentary, faunal and geochemical criteria developed from stratigraphic studies in NW Germany. In: Bhattacharji, S., et al. (Eds.), Global Bio-Events; A Critical Approach: Springer, Berlin 8, 345–351.

Holbourn, A., Kuhnt, W., 2002. Cenomanian–Turonian palaeoceanographic change on the Kerguelen Plateau: A comparison with Northern Hemisphere records. Cretaceous Research 23, 333–349.

Huber, B.T., Leckie, R.M., Norris, R.D., Bralower, T.J., CoBabe, E., 1999. Foraminiferal assemblage and stable isotopic change across the Cenomanian–Turonian boundary in the subtropical North Atlantic. Journal of Foraminiferal Research 29, 392–417.

Huber, B.T., Petrizzo, M.R., 2014. Evolution and taxonomic study of the Cretaceous planktic foraminiferal genus *Helvetoglobotruncana* Reiss, 1957. Journal of Foraminiferal Research 44, 40–57.

Huber, B.T., Petrizzo, M.R., Young, J.R., Falzoni, F., Gilardoni, S.E., Bown, P.R., Wade, B.S., 2016. Pforams@microtax: A new online taxonomic database for planktonic foraminifera. Micropaleontology 62, 429–438.

Huber, B.T., Petrizzo, M.R., Watkins, D.K., Haynes, S.J., MacLeod, K.G., 2017. Correlation of Turonian continental margin and deep-sea sequences in the subtropical Indian Ocean sediments by integrated planktonic foraminiferal and calcareous nannofossil biostratigraphy. Newsletters on Stratigraphy 50, 141–185.

Ion, J., 1976. A propos de la souche des Rotalipores, *Rotalipora praemontsalvensis* n.sp.: Dări de Seamă ale Şedinţelor, Institutul de Geologie şi Geofizică Bucharest 62, 39–46.

Jarvis, I., Carson, G.A., Cooper, M.K.E., Hart, M.B., Leary, P.N., Tocher, B.A., Horne, D., Rosenfeld, A., 1988. Microfossil assemblages and the Cenomanian–Turonian (Late Cretaceous) oceanic anoxic event. Cretaceous Research 9, 3–103.

Jarvis, I., Gale, A.S., Jenkyns, H.C., Pearce, M.A., 2006. Secular variation in Late Cretaceous carbon isotopes: A new $\delta^{13}C$ carbonate reference curve for the Cenomanian–Campanian (99.6–70.6 Ma). Geological Magazine 143, 561–608.

Jarvis, I., Lignum, J.S., Gröcke, D.R., Jenkyns, H.C., Pearce, M.A., 2011. Black shale deposition, atmospheric CO_2 drawdown, and cooling during the Cenomanian–Turonian Oceanic Anoxic Event. Paleoceanography 26, PA3201, doi:10.1029/2010PA002081.

Jenkyns, H.C., 2010. Geochemistry of oceanic anoxic events. Geochemistry, Geophysics, Geosystems 11, Q03004, doi:10.1029/2009GC002788.

Jenkyns, H.C., Dickson, A.J., Ruhl, M., Boorn, S.H., 2017. Basalt-seawater interaction, the Plenus Cold Event, enhanced weathering and geochemical change: Deconstructing Oceanic Anoxic Event 2 (Cenomanian–Turonian, Late Cretaceous). Sedimentology 64, 16–43.

Joo, Y.I., Sageman, B.B., 2014. Cenomanian to Campanian carbon isotope chemostratigraphy from the Western Interior Basin, U.S.A. Journal of Sedimentary Research 84, 529–542.

Kaiho, K., Katabuchi, M., Oba, M., Lamolda, M., 2014. Repeated anoxia-extinction episodes progressing from slope to shelf during the latest Cenomanian. Gondwana Research 25, 1357–1368.

Keller, G., Adatte, T., Berner, Z., Chellai, E.H., Stueben, D., 2008. Oceanic events and biotic effects of the Cenomanian-Turonian anoxic event, Tarfaya Basin, Morocco. Cretaceous Research 29, 976–994.

Keller, G., Berner, Z., Adatte, T., Stueben, D., 2004. Cenomanian–Turonian and $\delta^{13}C$, and $\delta^{18}O$, sea level and salinity variations at Pueblo, Colorado. Palaeogeography, Palaeoclimatology, Palaeoecology 211, 19–43.

Keller, G., Han, Q., Adatte, T., Burns, S., 2001. Paleoenvironment of the Cenomanian–Turonian transition at Eastbourne, England. Cretaceous Research 22, 391–422.

Keller, G., Pardo, A., 2004. Age and paleoenvironment of the Cenomanian–Turonian global stratotype section and point at Pueblo, Colorado. Marine Micropaleontology 51, 95–128.

Kennedy, W.J., Cobban, W.A., Elder, W.P., Kirkland, J.I., 1999. Lower Turonian (Upper Cretaceous) *Watinoceras devonense* Zone ammonite fauna in Colorado, USA. Cretaceous Research 20, 629–639.

Kennedy, W.J., Walaszczyk, I., Cobban, W.A., 2000. Pueblo, Colorado, USA, Candidate Global Boundary Stratotype Section and Point for the base of the Turonian Stage of the Cretaceous and for the Middle Turonian substage, with a revision of the Inoceramidae (Bivalvia). Acta Geologica Polonica 50, 295–334.

Kennedy, W.J., Walaszczyk, I., Cobban, W.A., 2005. The Global Boundary Stratotype Section and Point for the base of the Turonian Stage of the Cretaceous: Pueblo, Colorado, USA. Episodes 28, 93–104.

Kopaevich, L., Vishnevskaya, V., 2016. Cenomanian–Campanian (Late Cretaceous) planktonic assemblages of the Crimea–Caucasus area: Palaeoceanography, palaeoclimate and sea level changes. Palaeogeography, Palaeoclimatology, Palaeoecology 441, 493–515.

Kuhnt, W., Herbin, J.P., Thurow, J., Wiedmann, J., 1990. Distribution of Cenomanian–Turonian Organic Facies in the Western Mediterranean and along the adjacent Atlantic margin. In: Huc, A.Y. (Ed.), Deposition of Organic Facies. AAPG Studies in Geology 30, 133–160.

Kuhnt, W., Holbourn, A.E., Beil, S., Aquit, M., Krawczyk, T., Flögel, S., Chellai, E.H., Jabour, H., 2017. Unraveling the onset of Cretaceous Oceanic Anoxic Event 2 in an extended sediment archive from the Tarfaya–Laayoune Basin, Morocco. Paleoceanography 32, 923–946.

Kuhnt, W., Luderer, F., Nederbragt, S., Thurow, J., Wagner, T., 2005. Orbital-scale record of the late Cenomanian–Turonian oceanic anoxic event (OAE-2) in the Tarfaya Basin (Morocco). International Journal of Earth Sciences 94, 147–159.

Kuhnt, W., Nederbragt, A., Leine, L., 1997. Cyclicity of Cenomanian–Turonian organic-carbon-rich sediments in the Tarfaya Atlantic Coastal Basin (Morocco). Cretaceous Research 18, 587–601.

Lamolda, M.A., Gorostidi, A., Martínez, R., López, G., Peryt, D., 1997. Fossil occurrences in the Upper Cenomanian–Lower Turonian at Ganuza, northern Spain: An approach to Cenomanian/Turonian boundary chronostratigraphy. Cretaceous Research 18, 331–353.

Lamolda, M.A., Paul, C.R.C., Peryt, D., Pons, J.M., 2014. The Global Boundary Stratotype and Section Point (GSSP) for the base of the Santonian Stage," Cantera de Margas", Olazagutia, northern Spain. Episodes 37, 2–13.

Leckie, R.M., 1985. Foraminifera of the Cenomanian–Turonian boundary interval, Greenhorn Formation, Rock Canyon Anticline, Pueblo, Colorado. In: Pratt, L.M., Kauffman, E.G., Zelt, F.B. (Eds.), Fine-grained Deposits and Biofacies of the Cretaceous Western Interior Seaway: Evidence of Cyclic Sedimentary Processes, Field Trip Guidebook, Society of Economic Paleontologists and Mineralogists 4, 139–149.

Leckie, R.M., Bralower, T.J., Cashman, R., 2002. Oceanic anoxic events and plankton evolution: Biotic response to tectonic forcing during the mid-Cretaceous. Paleoceanography 17, doi:10.1029/2001PA000623.

Leckie, R.M., Yuretich, R.F., West, O.L.O., Finkelstein, D., Schmidt, M., 1998. Paleoceanography of the southwestern Western Interior Sea during the time of the Cenomanian–Turonian boundary (Late Cretaceous). In: Dean, W., Arthur, M.A. (Eds.), Stratigraphy and Paleoenvironments of the Cretaceous Western Interior Seaway. SEPM Concepts in Sedimentology and Paleontology 6, 101–126.

Lipson-Benitah, S., Rosenfeld, A., Akira Flexer, A.H., Kashai, E., 1988. The middle Turonian Daliyya type section in Israel: Biostratigraphy, palaeoenvironment and sea-level changes. Cretaceous Research 9, 321–336.

Lirer, F., 2000. A new technique for retrieving calcareous microfossils from lithified lime deposits. Micropaleontology 46, 365–369.

Longoria, J.F., 1973. *Pseudoticinella*, a new genus of planktonic foraminifera from the early Turonian of Texas. Revista Española de Micropaleontología 5, 417–423.

Lowery, C.M., Corbett, M.J., Leckie, R.M., Watkins, D., Miceli Romero, A., Pramudito, A., 2014. Foraminiferal and nannofossil paleoecology and paleoceanography of the Cenomanian–Turonian Eagle Ford Shale of southern Texas. Palaeogeography, Palaeoclimatology, Palaeoecology 413, 49–65.

Lowery, C.M., Leckie, R.M., 2017. Biostratigraphy of the Cenomanian-Turonian Eagle Ford Shale of South Texas. Journal of Foraminiferal Research 47, 105–128.

Luciani, V., Cobianchi, M., 1999. The Bonarelli Level and other black shales in the Cenomanian–Turonian of the northeastern Dolomites (Italy): calcareous nannofossil and foraminiferal data. Cretaceous Research 20, 135–167.

Luderer, F., Kuhnt, W., 1997. A high resolution record of the *Rotalipora* extinction in laminated organic-carbon rich limestones of the Tarfaya Atlantic coastal basin (Morocco). Ann. Soc. Géol. Nord (2eme Sér.) 5, 199–205.

MacLeod, N., Keller, G., 1991. How complete are Cretaceous/Tertiary boundary sections? A chronostratigraphic estimate based on graphic correlation. Geological Society of America Bulletin 103, 1439–1457.

Meyers, S.R., Sageman, B.B., Hinnov, L.A., 2001. Integrated quantitative stratigraphy of the Cenomanian–Turonian Bridge Creek Limestone Member using evolutive

harmonic analysis and stratigraphic modeling. Journal of Sedimentary Research 71, 628–644.
Meyers, S.R., Siewert, S.E., Singer, B.S., Sageman, B.B., Condon, D.J., Obradovich, J.D., Jicha, B.R., Sawyer, D.A., 2012. Intercalibration of radioisotopic and astrochronologic time scales for the Cenomanian–Turonian boundary interval, Western Interior Basin, USA. Geology 40, 7–10.
Morrow, A.L., 1934. Foraminifera and Ostracoda from the Upper Cretaceous of Kansas. J. Paleontol. 8, 186–205.
Mort, H., Jacquat, O., Adatte, T., Steinmann, P., Föllmi, K., Matera, V., Berner, Z., Stüben, D., 2007. The Cenomanian/Turonian anoxic event at the Bonarelli Level in Italy and Spain: Enhanced productivity and/or better preservation? Cretaceous Research 28, 597–612.
Nederbragt, A.J., Fiorentino, A., 1999. Stratigraphy and palaeoceanography of the Cenomanian–Turonian Boundary Event in Oued Mellegue, north-western Tunisia. Cretaceous Research 20, 47–62.
Olayiwola, M.A., Bamford, M.K., Durugbo, E.U., 2017. Graphic correlation: A powerful tool for biostratigraphic correlation of petroleum exploration and production in the Cenozoic deep offshore Niger Delta, Nigeria. Journal of African Earth Sciences 131, 156–165.
Pagani, M., Arthur, M.A., 1998. Stable isotopic studies of the Cenomanian–Turonian proximal marine fauna from the U.S. Western Interior Seaway. In: Dean, W.E., Arthur, M.A. (Eds.), SEPM Concepts in Sedimentology and Paleontology, vol.6. SEPM, Tulsa, USA, pp.201–225.
Paul, C.R.C., Lamolda, M.A., 2009. Testing the precision of bioevents. Geological Magazine 146, 625–637.
Paul, C.R.C., Lamolda, M.A., Mitchell, S.F., Vaziri, M.R., Gorostidi, A., Marshall, J.D., 1999. The Cenomanian–Turonian boundary at Eastbourne (Sussex, UK): A proposed European reference section. Palaeogeography, Palaeoclimatology, Palaeoecology 150, 83–121.
Pearce, M.A., Jarvis, I., Tocher, B.A., 2009. The Cenomanian–Turonian boundary event, OAE2 and palaeoenvironmental change in epicontinental seas: New insights from the dinocyst and geochemical records. Palaeogeography, Palaeoclimatology, Palaeoecology 280, 207–234.
Pessagno, E.A., Jr., 1967. Upper Cretaceous planktonic foraminifera from the western Gulf Coastal Plain. Paleontographica Americana 5, 245–445.
Petrizzo, M.R., 2000. Upper Turonian–lower Campanian planktonic foraminifera from southern mid–high latitudes (Exmouth Plateau, NW Australia): biostratigraphy and taxonomic notes. Cretaceous Research 21, 479–505.
Petrizzo, M.R., 2001. Late Cretaceous planktonic foraminifera from Kerguelen Plateau (ODP Leg 183): New data to improve the Southern Ocean biozonation: Cretaceous Research 22, 829–855.
Petrizzo, M.R., 2002. Palaeoceanographic and palaeoclimatic inferences from Late Cretaceous planktonic foraminiferal assemblages from the Exmouth Plateau (ODP Sites 762 and 763, eastern Indian Ocean). Marine Micropaleontology 45, 117–150.
Petrizzo, M.R., Falzoni, F., Premoli Silva, I., 2011. Identification of the base of the lower-to-middle Campanian *Globotruncana ventricosa* Zone: Comments on reliability and global correlations. Cretaceous Research 32, 387–405.
Petrizzo, M.R., Jiménez Berrocoso, Á., Falzoni, F., Huber, B.T., MacLeod, K.G., 2017. The Coniacian–Santonian sedimentary record in southern Tanzania (Ruvuma Basin, East Africa): Planktonic foraminiferal evolutionary, geochemical and palaeoceanographic patterns. Sedimentology 64, 252–285.
Pratt, L.M., 1984. Influence of paleoenvironmental factors on preservation of organic matter in Middle Cretaceous Greenhorn Formation, Pueblo, Colorado. AAPG Bulletin 68, 1146–1159.
Pratt, L.M., 1985. Isotopic studies of organic matter and carbonate in rocks of the Greenhorn marine cycle. In: Pratt, L.M., Kauffman, E.G., Zelt, F.B. (Eds.), Fine-grained Deposits and Biofacies of the Cretaceous Western Interior Seaway: Evidence of Cyclic Sedimentary Processes, Field Trip Guidebook, Society of Economic Paleontologists and Mineralogists 4, 38–48.
Pratt, L.M., Arthur, M.A., Dean, W.E., Scholle, P.A. 1993. Paleo-oceanographic cycles and events during the Late Cretaceous in the Western Interior Seaway of North America. In: Caldwell, W.G.E., Kauffman, E.G. (Eds.), Geological Association of Canada Special Paper 39, 333–353.
Pratt, L.M., Threlkeld, C.N., 1984. Stratigraphic significance of $^{13}C/^{12}C$ ratios in mid-Cretaceous rocks of the Western Interior. Memoir of the Canadian Society of Petroleum Geologists 9, 305–312.
Premoli Silva, I., Sliter, W.V., 1995. Cretaceous planktonic foraminiferal biostratigraphy and evolutionary trends from the Bottaccione section, Gubbio, Italy. Palaeontographia Italica 81, 2–90.
Premoli Silva, I., Erba, E., Salvini, G., Locatelli, C., Verga, D., 1999. Biotic changes in Cretaceous oceanic anoxic events of the Tethys. Journal of Foraminiferal Research 29, 352–370.
Premoli Silva, I., Sliter, W.V., 1999. Cretaceous paleoceanography: Evidence from planktonic foraminiferal evolution. In: Barrera, E., Johnson, C.C., (Eds.), The Evolution of the Cretaceous Ocean-Climate System. Special Papers of the Geological Society of America 332, 301–328, doi: 10.1130/0-8137-2332-9.301.
Robaszynski, F., Caron, M., 1995. Foraminiféres planctoniques du Crétacé: commentaire de la zonation Europe-Méditerranée. Bulletin de la Société Géologique de France 166, 681–692.
Robaszynski, F., Caron, M., le Groupe de Travail Européen des Foraminifères Planctoniques, 1979. Atlas des Foraminifères Planctoniques du Crétacé Moyen (Mer Boréale et Téthys). Cahiers de Micropaléontologie 1, 1–185; 2, 1–181.
Robaszynski, F., Caron, M., Amédro, F., Dupuis, C., Hardenbol, J., González-Donoso, J.M., Linares, D., Gartner, S., 1993. Le Cénomanien de la region de Kalaat Senan (Tunisie Centrale): litho-biostratigraphie et interpretation séquentielle. Revue de Paléobiologie 12, 351–505.

Robaszynski, F., Caron, M., Dupuis, C., Amédro, F., González-Donoso, J.M., Linares, D., Hardenbol, J., Gartner, S., Calandra, F., Deloffre, R., 1990. A tentative integrated stratigraphy in the Turonian of Central Tunisia: formations, zones and sequential stratigraphy in the Kalaat Senan area. Bulletin des Centres de Recherches Exploration-Production Elf Aquitaine 14, 213–384.

Robaszynski, F., Gale, A., Juignet, P., Amédro, F., Hardenbol, J., 1998. Sequence stratigraphy in the Upper Cretaceous series of the Anglo-Paris Basin: exemplified by the Cenomanian stage. In: de Graciansky, P.-C. et al. (Eds.), Mesozoic and Cenozoic sequence stratigraphy of European Basins. SEPM Special Publications 60, 363–386.

Sadler, P.M., 2004. Quantitative biostratigraphy-Achieving finer resolution in global correlation. Annual Review Earth and Planetary Sciences 32, 187–213.

Sageman, B.B., Meyers, S.R., Arthur, M.A., 2006. Orbital time scale and new C-isotope record for Cenomanian–Turonian boundary stratotype. Geology 34, 125–128.

Schlanger, S.O., Arthur, M.A., Jenkyns, H.C., Scholle, P.A., 1987. The Cenomanian–Turonian Oceanic Anoxic Event, I. Stratigraphy and distribution of organic carbon-rich beds and the marine $\delta^{13}C$ excursion. Geological Society, London, Special Publications 26, 371–399.

Schlanger, S.O., Jenkyns, H.C., 1976. Cretaceous oceanic anoxic events: Causes and consequences. Geologie en Mijnbouw 55, 179–184.

Scholle, P.A., Arthur, M.A., 1980. Carbon isotope fluctuations in Cretaceous pelagic limestones: Potential stratigraphic and petroleum exploration tool. American Association of Petroleum Geologists Bulletin 64, 67–87.

Scopelliti, G., Bellanca, A., Coccioni, R., Luciani, V., Neri, R., Baudin, F., Chiari, M., Marcucci, M., 2004. High-resolution geochemical and biotic records of the Tethyan "Bonarelli Level" (OAE2, latest Cenomanian) from the Calabianca–Guidaloca composite section, northwestern Sicily, Italy. Palaeogeography, Palaeoclimatology, Palaeoecology 208, 293–317.

Shaw, A.B., 1964. Time in stratigraphy. McGraw-Hill, New York, USA, 365 pp.

Sinninghe Damsté, J.S., van Bentum, E.C., Reichart, G.J., Pross, J., Schouten, S., 2010. A CO_2 decrease-driven cooling and increased latitudinal temperature gradient during the mid-Cretaceous Oceanic Anoxic Event 2. Earth and Planetary Science Letters 293, 97–103.

Sliter, W.V., 1989. Biostratigraphic zonation for Cretaceous planktonic foraminifers examined in thin section. The Journal of Foraminiferal Research 19, 1–19.

Smith, A.G., Barry, T., Bown, P., Cope, J., Gale, A., Gibbard, P., Gregory, J., Hounslow, M., Kemp, D., Knox, R., Marshall, J., Oates, M., Rawson, P., Powell, J., Waters, C., 2015. GSSPs, global stratigraphy and correlation. In: Smith, D.G., et al. (Eds), Strata and Time: Probing the Gaps in Our Understanding. Geological Society, London, Special Publications 404, 37–67.

Tsikos, H., Jenkyns, H.C., Walsworth-Bell, B., Petrizzo, M.R., Forster, A., Kolonic, S., Erba, E., Premoli Silva, I., Baas, M., Wagner, T., Sinninghe Damsté, J.S., 2004. Carbon-isotope stratigraphy recorded by the Cenomanian–Turonian Oceanic Anoxic Event: Correlation and implications based on three localities. Journal of the Geological Society of London 161, 711–719.

Tur, N.A., Smirnov, J.P., Huber, B.T., 2001. Late Albian–Coniacian planktic foraminifera and biostratigraphy of the northeastern Caucasus: Cretaceous Research 22, 719–734.

Voigt, S., Aurag, A., Leis, F., Kaplan, U., 2007. Late Cenomanian to Middle Turonian high-resolution carbon isotope stratigraphy: New data from the Münsterland Cretaceous Basin, Germany. Earth and Planetary Science Letters 253, 196–210.

Voigt, S., Erbacher, J., Mutterlose, J., Weiss, W., Westerhold, T., Wiese, F., Wilmsen, M., Wonik, T., 2008. The Cenomanian–Turonian of the Wunstorf section – (North Germany): Global stratigraphic reference section and new orbital time scale for Oceanic Anoxic Event 2. Newsletters on Stratigraphy 43, 65–89.

West, O.L., Leckie, R.M., Schmidt, M., 1998. Foraminiferal paleoecology and paleoceanography of the Greenhorn cycle along the southwestern margin of the Western Interior Sea. SEPM, Concepts in Sedimentology and Paleontology 6, 79–99.

Westermann, S., Caron, M., Fiet, N., Fleitmann, D., Matera, V., Adatte, T., Föllmi, K.B., 2010. Evidence for oxic conditions during oceanic anoxic event 2 in the northern Tethyan pelagic realm. Cretaceous Research 31, 500–514.

Wonders, A.A.H., 1980. Middle and Late Cretaceous planktonic foraminifera of the western Mediterranean area. Utrecht Micropaleontological Bulletin 24, 1–157.

Manuscript received: July 14, 2017
Revisions required: September 19, 2017
Revised version received: November 15, 2017
Manuscript accepted: November 24, 2017

Taxonomic Appendix

The genus "*Heterohelix*" is quoted because the taxonomy of this group is currently under revision by the Mesozoic Planktonic Foraminiferal Working Group. Specifically, all biserial taxa occurring across the C–T boundary interval were traditionally included in the genus *Heterohelix*, but more recent taxonomic studies highlighted the occurrence of a number of different phyletic lineages, thus different genera (e.g., Georgescu 2007, Georgescu and Huber 2009, Haynes et al. 2015). So, while we have maintained the term "*Heterohelix*" shift to be consistent with previous authors, it should be noted that all biserial species occurring across the C/T boundary are presently accommodated in other genera (e.g., *Protoheterohelix*, *Planoheterehelix*, *Huberella*).

List of planktonic foraminiferal species with authors and years mentioned in the text and/or in the figures.

Dicarinella canaliculata (Reuss, 1854)
Dicarinella elata Lamolda, 1977
Dicarinella hagni (Scheibnerova, 1962)
Dicarinella imbricata (Mornod, 1950)
Falsotruncana maslakovae Caron, 1981
"Globigerinelloides" bentonensis (Morrow, 1934). The genus *Globigerinelloides* is herein indicated in brackets, as it is currently under revision by the Mesozoic Planktonic Foraminiferal Working Group; see Taxonomic notes in Petrizzo et al. (2017).
Helvetoglobotruncana helvetica (Bolli, 1945)
Helvetoglobotruncana praehelvetica (Trujillo, 1960)
Laeviheterohelix pulchra (Brotzen, 1936)
Marginotruncana coronata (Bolli, 1945)
Marginotruncana marianosi (Douglas, 1969)
Marginotruncana renzi (Gandolfi, 1942)
Marginotruncana schneegansi (Sigal, 1952)
Marginotruncana sigali (Reichel, 1950)
Planoheterohelix globulosa (Ehrenberg, 1840)
Planoheterohelix moremani (Cushman, 1938)
Planoheterohelix paraglobulosa (Georgescu and Huber, 2009)
Planoheterohelix reussi (Cushman, 1938)
Praeglobotruncana algeriana Caron, 1966
Praeglobotruncana oraviensis Scheibnerova, 1960
Rotalipora cushmani (Morrow, 1934)
Rotalipora montsalvensis (Mornod, 1950)
Rotalipora praemontsalvensis Ion, 1976
Rotalipora planoconvexa (Longoria, 1973)
Thalmanninella brotzeni Sigal, 1948
Thalmanninella deeckei (Franke, 1925)
Thalmanninella globotruncanoides (Sigal, 1948)
Thalmanninella greenhornensis (Morrow, 1934)
Thalmanninella multiloculata (Morrow, 1934)
Whiteinella aprica (Loeblich and Tappan, 1961)
Whiteinella archaeocretacea Pessagno, 1967
Whiteinella brittonensis (Loeblich and Tappan, 1961)

Supplementary materials

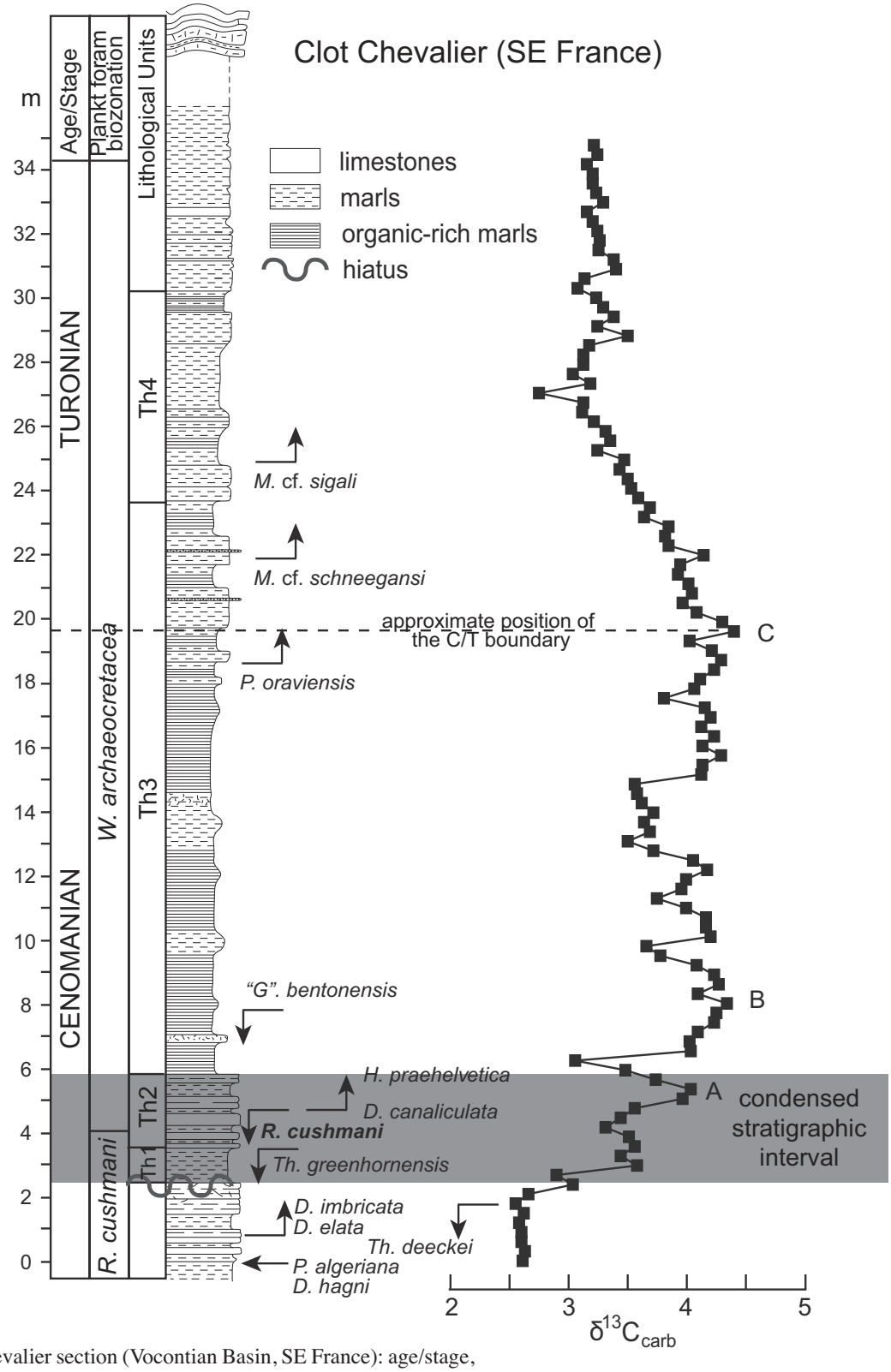

Figure A. Clot Chevalier section (Vocontian Basin, SE France): age/stage, lithostratigraphy, planktonic foraminiferal biostratigraphy and bioevents, $\delta^{13}C_{carb}$ profile and chemostratigraphic events after Falzoni et al. (2016b).

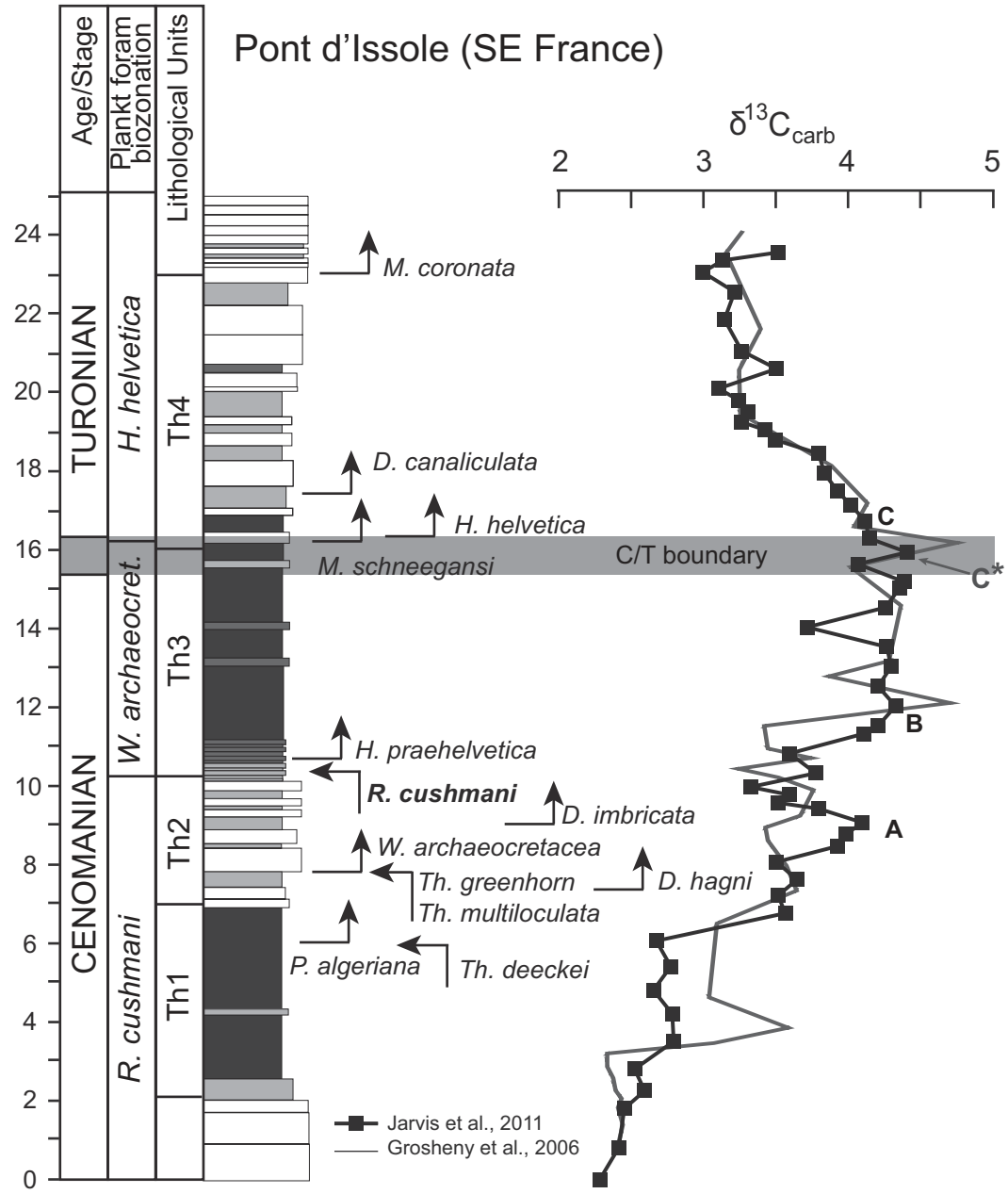

Figure B. Pont d'Issole section (Vocontian Basin, SE France): the chemostratigraphic events are after Jarvis et al. (2011), with the exception of peak C (grey with * in this figure) that is herein placed based on the definition given in the text. The position of the C/T boundary is here estimated to fall within the interval from the estimated LO of *W. devonense* based on the bio- and chemostratigraphic correlation with Eastbourne (see Jarvis et al. 2011) and the LO of *H. helvetica* and includes peak C (as positioned in this study). Lithostratigraphy is according to Jarvis et al. (2011). Planktonic foraminiferal biostratigraphy and bioevents are from Grosheny et al. (2006). The $\delta^{13}C_{carb}$ profiles are from Grosheny et al. (2006) and Jarvis et al. (2011).

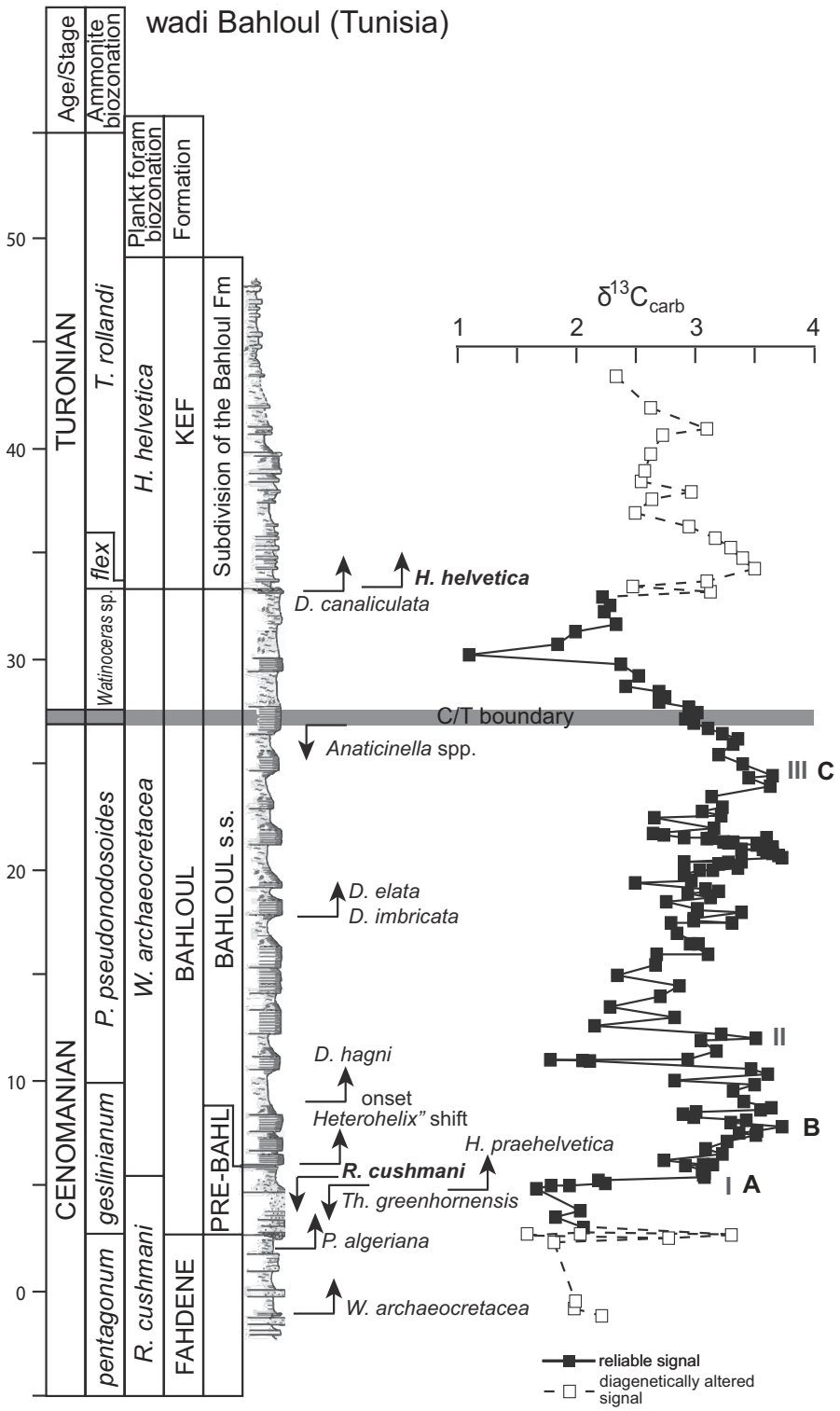

Figure C. Wadi Bahloul section (Tunisia): age/stage, lithostratigraphy, ammonite zonation, planktonic foraminiferal biostratigraphy and bioevents, $\delta^{13}C_{carb}$ profile and chemostratigraphic events (I, II, and III) from Caron et al. (2006). A, B, and C peaks are here placed according to the definition provided in this study.

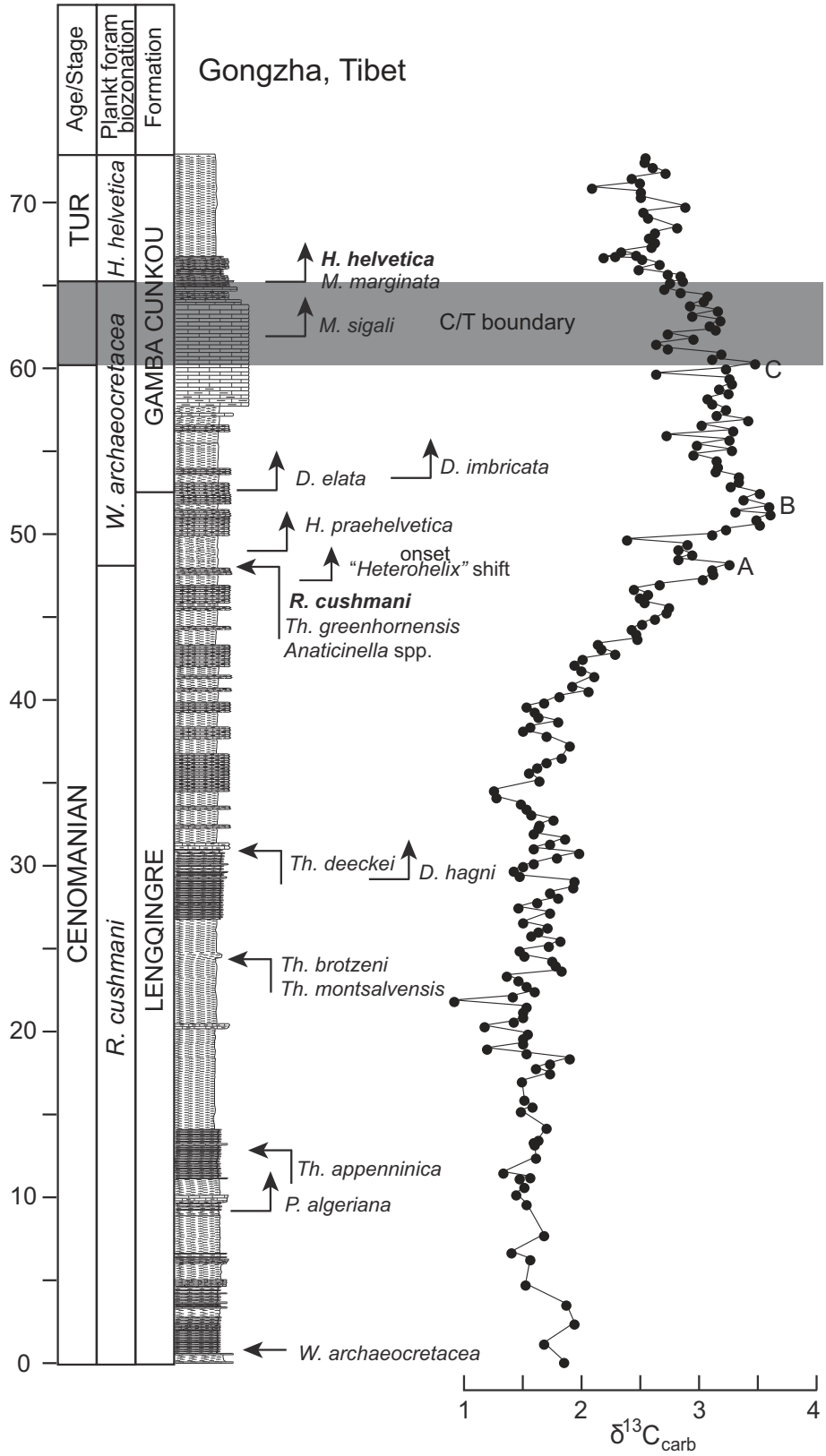

Figure D. Gongzha section (Tibet): formations, planktonic foraminiferal biostratigraphy and bioevents, $\delta^{13}C_{carb}$ profile and chemostratigraphic events from Bomou et al. (2013). The position of the C/T boundary is here estimated to fall within the interval from peak C and the LO of *H. helvetica*.

References

Bomou, B., Adatte, T., Tantawy, A.A., Mort, H., Fleitmann, D., Huang, Y., Föllmi, K.B., 2013. The expression of the Cenomanian–Turonian oceanic anoxic event in Tibet. Palaeogeography, Palaeoclimatology, Palaeoecology 369, 466–481.

Caron, M., Dall'Agnolo, S., Accarie, H., Barrera, E., Kauffman, E.G., Amédro, F., Robaszynski, F., 2006. High-resolution stratigraphy of the Cenomanian–Turonian boundary interval at Pueblo (USA) and wadi Bahloul (Tunisia): Stable isotope and bio-events correlation. Géobios 39, 171–200.

Falzoni, F., Petrizzo, M.R., Jenkyns, H.C., Gale, A.S., Tsikos, H., 2016b. Planktonic foraminiferal biostratigraphy and assemblage composition across the Cenomanian–Turonian boundary interval at Clot Chevalier (Vocontian Basin, SE France). Cretaceous Research, 59, 69–97.

Grosheny, D., Beaudoin, B., Morel, L., Desmares, D., 2006. High-resolution biostratigraphy and chemostratigraphy of the Cenomanian–Turonian Boundary Event in the Vocontian Basin, S-E France. Cretaceous Research 27, 629–640.

Jarvis, I., Lignum, J.S., Gröcke, D.R., Jenkyns, H.C., Pearce, M.A., 2011. Black shale deposition, atmospheric CO_2 drawdown, and cooling during the Cenomanian–Turonian Oceanic Anoxic Event. Paleoceanography 26, PA3201, doi:10.1029/2010PA002081.